arXiv:1611.06766v1 [math.OC] 21 Nov 2016

Sufficient Optimality Conditions for Distributed, Non-Predictive Ramp Metering in the Monotonic Cell Transmission Model*

Marius Schmitt, Chithrupa Ramesh, and John Lygeros†

November 22, 2016

Abstract

We consider the freeway ramp metering problem, based on the Cell Transmission Model. Assuming perfect model knowledge and perfect traffic demand prediction, the ramp metering problem can be cast as a finite horizon optimal control problem with the objective of minimizing the Total Time Spent, i.e., the sum of the travel times of all drivers. For this reason, the application of Model Predictive Control (MPC) to the ramp metering problem has been proposed. However, practical tests on freeways show that MPC rarely outperforms simple, decentralized feedback strategies. Until now, a theoretical justification for this empirical observation is lacking. This work compares the performance of distributed, non-predictive feedback strategies to the optimal solution. To do so, we propose a distributed, non-predictive controller, and show that this controller preserves monotonicity of the closed-loop system. We exploit this result to derive sufficient conditions under which the distributed controller achieves globally optimal performance. In a small case study based on real-world traffic data, we also demonstrate that these optimality conditions are rarely violated on a typical day. In addition, even in cases when they are violated, the performance deterioration is shown to be negligibly small.

1 Introduction

Ramp metering refers to the active control of the inflow of cars on a freeway via the onramps, by means of installing and controlling a traffic light at every onramp. In this work, we consider the freeway ramp metering problem over a finite horizon, e.g. one day or one rush-hour period. Freeway ramp metering has been established as an effective and practically useful tool to improve traffic flows on congestion-prone freeways [14, 16]. We study the problem by adopting the Cell Transmission Model (CTM) for freeways, as introduced in the seminal work by Daganzo [3, 4], which can be interpreted as a first-order Godunov approximation of the continuous Lighthill-Whitham-Richards-model (LWR) [9, 21]. The popularity of the CTM for model-based control stems from the simplicity of the model equations, allowing for computationally efficient solutions methods for optimal control problems [6, 28] and the fact that the CTM might be regarded as more realistic than some competing models, since it never predicts negative velocities for freeway traffic. Modifications and generalizations of this model have since been introduced, and we consider a slight generalization of the original, piece-wise affine CTM to a more general, concave fundamental diagram as defined and analyzed in [10]. Furthermore, we employ a simplified onramp model originally introduced as the "asymmetric" CTM [6, 7], which simplifies the model of onramp-mainline merges by distinguishing mainline- and onramp-traffic demand.

While tractable model-based, optimal-control strategies have been proposed [6, 20, 1, 2], a conceptually different approach uses distributed or even completely decentralized feedback. In such ramp metering strategies, local controllers only receive measurements from sensors in close vicinity to a particular onramp location and only exchange limited amounts of information, preferably with adjacent controllers if at all [15, 24, 27]. Those control policies aim at maximizing bottleneck flows locally, but have been shown to come close to the performance of optimal ramp metering strategies in real-world evaluations [23, 25, 19]. While it is apparent

*Research was supported by the European Union 7th Framework Program "Scalable Proactive Event-Driven Decision-making (SPEEDD)" (FP7-ICT 619435).

†[1]Automatic Control Laboratory, ETH Zurich, Switzerland, <schmittm,rameshc,lygeros>@control.ee.ethz.ch

that such local feedback controllers are far easier to implement than model-based optimal control strategies, it is not obvious why and when the performance of distributed, non-predictive ramp metering strategies comes close to the centralized optimal control solution. A special case for which the optimal control strategy can be explicitly constructed is analyzed in [26]. It is stated that the structure of the explicit solution "explains why some local metering algorithms [...] are successful – they are really close to the most-efficient logic". However, no proof of optimality is provided.

This work addresses the question of how distributed, non-predictive ramp metering policies compare to optimal, centralized and predictive control strategies for freeways modeled by the monotonic CTM. If perfect model knowledge and perfect traffic demand prediction is assumed, the ramp metering problem can be cast as a finite horizon optimal control problem with the objective of minimizing the Total Time Spent. It is known that this problem can be reformulated as a convex optimization problem for monotonic demand and supply functions in the fundamental diagram [10] and as a Linear Program in the case of a piecewise-affine fundamental diagram [6]. Since perfect model knowledge and in particular perfect traffic demand prediction seem to be unrealistic (see e.g. [2, 12, 13] for ongoing work to mitigate the challenges involved), we introduce a local feedback controller for freeway ramp metering instead. This controller performs a distributed, one step ahead maximization of local traffic flows.Exploiting monotonicity of the CTM, we derive sufficient optimality conditions for the problem of minimizing the Total Time Spent (TTS), which is defined as the sum of the travel times of all drivers.

We analyze performance in a case study, based on a real-world freeway described in [5]. The study is conducted using the monotonic CTM, with freeway parameters and demand patterns estimated from real measurements. Even though the optimality conditions are occasionally violated, the control performance of the centralized optimal controller and the proposed ideal non-predictive, distributed controller differ only by fractions of percents in simulations based on the CTM. Finally, analyzing differences between the CTM and reality allows us to identify key issues that have to be addressed by control strategies that aim at outperforming existing, distributed feedback controllers for ramp metering in the real world.

To sum up, the main contributions of this paper are:

- We derive sufficient optimality conditions for minimal TTS ramp metering in the CTM, providing a thorough theoretical assessment of why (and when) performance of distributed controllers and optimal control strategies may coincide.
- We demonstrate the usefulness of these conditions by defining a suitable distributed, non-predictive feedback controller, which achieves nearly optimal control performance for simulations of the CTM, using real-world parameters and traffic demands.

Section 2 defines the CTM and the main problem of minimizing TTS. In Section 3, we introduce a non-predictive, distributed controller for ramp metering. We also show that this controller is not always optimal, by stating two counterexamples. In Section 4, we derive sufficient optimality conditions that can be used to check optimality a posteriori. Section 5 introduces a case study based on real-world freeway parameters, and we demonstrate that the performance deterioration of distributed, best-effort control is negligibly small. Finally, in Section 6, we comment on the implications of the results, and highlight immediate consequences for the development of real-world, predictive, coordinated ramp-metering strategies.

We adopt the following notation: The k-th component of a vector x is denoted x_k. The index k will always be used to denote the index of a cell in the CTM and hence $k \in \{1, \dots, n\}$ with n the number of cells in the model, unless a different range is explicitly specified. If a variable x evolves over time, the value at time t is denoted by $x(t)$. We consider discrete time models over a horizon T, i.e., $t \in \{0, \dots, T\}$. The operators $\leq, \geq, <, >$ used with vectors denote elementwise inequalities. Also, we write $[x]_l^u := \min\{u, \max\{x, l\}\}$ for a saturation at an upper bound u and lower bound l.

2 Problem formulation

The original CTM was introduced in [3, 4]. We consider the (asymmetric) CTM as introduced in [6, 7], which employs a simplified onramp model, as visualized in Figure 1. In the CTM, the freeway is partitioned into *cells* of length l_k. The state of the mainline is described by the traffic *density* $\rho_k(t)$, i.e., the number of cars per length in each cell. The metered onramps are modeled as integrators, and their state is given by the

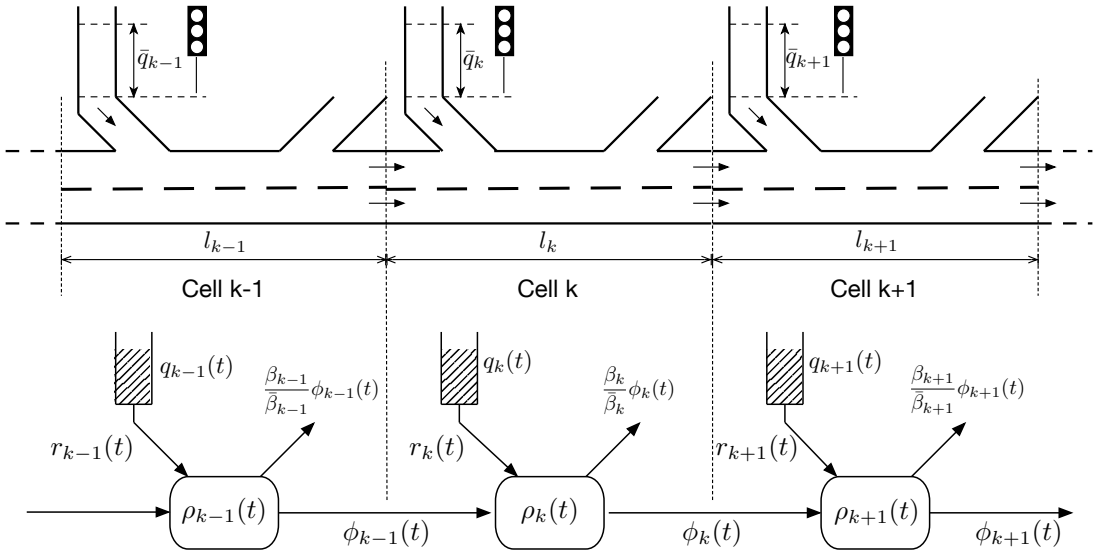

Figure 1: Sketch of the CTM of a freeway segment controlled by ramp metering

queue length $q_k(t)$, i.e., the number of cars waiting in the queue. The evolution of the system is described by flows of cars during discrete time intervals of duration Δt. The mainline *flow* between cells k and $k+1$ in time interval t is denoted by $\phi_k(t)$. We make the assumption of constant split ratios, which means that the outflows from the offramps are modeled as percentages β_k of the mainline flows, where β_k are designated as the *split ratios* of traffic at the offramp in cell k. For notational convenience, we also use $\bar{\beta}_k := 1 - \beta_k$. For metered onramps, the inflows to the freeway are given by the ramp *metering rates* $r_k(t)$. The *external traffic demands* $w_k(t)$, i.e., the number of cars per unit time seeking to enter the freeway from either a ramp $k \in \{1, \ldots, n\}$ or from the upstream mainline, act as external disturbances on the system. The evolution of the state of the CTM is described by the conservation laws

$$\rho_k(t+1) = \rho_k(t) + \frac{\Delta t}{l_k}\left(\phi_{k-1}(t) + r_k(t) - \frac{1}{\bar{\beta}_k}\phi_k(t)\right), \tag{1a}$$

$$q_k(t+1) = q_k(t) + \Delta t \cdot (w_k(t) - r_k(t)). \tag{1b}$$

The metering rates $r_k(t)$ serve as control inputs to the system. The onramp model relies on the implicit assumption that congestion does not spill back onto the onramps. In particular, the model assumes that all cars assigned to enter the freeway in a sampling interval can indeed do so. While this assumption might not be satisfied for an uncontrolled freeway, it was shown to be satisfied for a freeway controlled by ramp metering in a case study [6]. In this study, the upper bounds on the metering rates as determined by the mainline congestion exceeded the actual metering rates by a large margin. Naturally, the ramp metering rates are nonnegative and also subject to a constant upper bound

$$0 \le r_k(t) \le \bar{r}_k, \tag{2}$$

which characterizes the finite maximal onramp flow. We will assume that the external demand is bounded $0 \le w_k(t) \le \bar{r}_k$ for all k and for all times t. In addition, the limited space on the onramp $0 \le q_k(t) \le \bar{q}_k(t)$ potentially limits the allowed ramp metering rates further and using (1b), we obtain bounds

$$\frac{1}{\Delta t}\left(q_k(t) - \bar{q}_k\right) + w_k(t) \le r_k(t) \le \frac{1}{\Delta t}q_k(t) + w_k(t) \tag{3}$$

in terms of the metering rates. The upper bound simply ensures that only cars seeking admission in time interval t can be admitted to enter the freeway, while the lower bound mandates that the ramp is operated

such that the queue length on the onramp never exceeds the length of the ramp, to avoid queue spill back[1]. We do not impose similar bounds on the outflows via the offramps: Effects like a spill back of congestion from the adjacent aterials are beyond the scope of this model and a constant, upper bound on the outflow from an offramp is redundant under the assumption of constant split ratios.

The CTM is a first order model and therefore, the mainline traffic flows $\phi(t)$ are not states but functions of the densities. The mainline flow $\phi_k(t)$ depends on the traffic *demand* $d_k(\rho_k(t))$ proportional to the number of cars that seek to travel downstream from cell k at time t, and the *supply* $s_{k+1}(\rho_{k+1}(t))$ of free space available downstream in cell $k+1$ at time t. Demand- and supply functions are often identified as the *fundamental diagram* of a cell, as depicted in Figure 2. In the original work of [3, 4], a piecewise-affine (PWA) fundamental diagram was assumed, as it is obtained from the Godunov discretization of the LWR-model. In practice, one might want to consider more general shapes of the fundamental diagram and hence of the demand- and supply functions, in order to better approximate real world data (see e.g. [8, 10] for recent examples). In the remainder of this work, we will assume that:

Assumption 1. *For every cell k, define a maximal density $\bar{\rho}_k$, often called the jam density, and the critical density $0 < \rho_k^c < \bar{\rho}_k$. The demand $d_k(x)$, $d_k : [0, \bar{\rho}] \to \mathbb{R}_+$ is a Lipschitz-continuous, nondecreasing function with $d_k(0) = 0$ and $d_k(\rho_k^c) = d_k(\bar{\rho}_k)$. Conversely, the supply $s_k(x)$, $s_k : [0, \bar{\rho}] \to \mathbb{R}_+$ is a Lipschitz-continuous, nonincreasing function with $s_k(\bar{\rho}) = 0$ and $s_k(\rho_k^c) = s_k(0)$. Furthermore, the sampling time Δt is chosen such that it satisfies the bounds*

$$\Delta t \cdot c_k^d \leq l_k \bar{\beta}_k \quad \forall k, \tag{4a}$$

$$\Delta t \cdot c_k^s \leq l_k \quad \forall k, \tag{4b}$$

with respect to the Lipschitz constants of the demand c_k^d and of the supply c_k^s.

The flow

$$\phi_0(t) = w_0(t), \tag{5a}$$

$$\phi_k(t) = \min\{d_k(\rho_k(t)), s_{k+1}(\rho_{k+1}(t))\} \quad \forall k \in \{1, \dots, n-1\}, \tag{5b}$$

$$\phi_n(t) = d_n(\rho_n(t)), \tag{5c}$$

is now given as the minimum of upstream demand and downstream supply. Note that the assumption of monotonicity of the demand functions implies that $d_k(\rho_k) = d_k(\rho_k^c)\ \forall\ \rho_k : \rho_k^c \leq \rho_k \leq \bar{\rho}_k$, i.e., the traffic demand is constant for densities larger than the critical density. Similarly, the assumption on monotonicity of the supply function implies that the supply is constant for all densities smaller than the critical density, i.e., $s_k(\rho_k) = s_k(\rho_k^c)\ \forall\ \rho_k : 0 \leq \rho_k \leq \rho_k^c$. It is sometimes helpful to introduce the maximal flow $F_k := \min\{d_k(\rho_k^c), s_{k+1}(\rho_{k+1}^c)\}$ as an additional parameter in the flow equations. The flow equation (5b) can then equivalently be written as

$$\phi_k(t) = \min\{d_k(\rho_k(t)), F_k, s_{k+1}(\rho_{k+1}(t))\}.$$

We will use F_k in the flow equations only when it simplifies the presentation of a proof or of an example. The flow equations are slightly modified for the first and the last cell. For the last cell, we assume that the outflow from the freeway is unobstructed, i.e., no congestion exists downstream of the (part of the) freeway that is modeled. Similarly, the inflow in the first cell is given by the external traffic demand $w_0(t)$, which is *not* restricted by the supply in the first cell. The reason for this modification is that the flow into the first cell arises from external traffic demand. The equations therefore ensure that all external demand eventually will be served. By contrast, limiting the inflow according to the supply of free space, as it is done for any internal flow, would amount to discarding the surplus external demand. It is worth emphasizing that local traffic flows (5) are maximized at the critical density. In particular, the flow ϕ_k into some cell $k+1$ with density equal to or smaller than the critical density $\rho_{k+1}(t) \leq \rho_{k+1}^c$ is not constrained by the supply of free space and hence $\phi_k(t) = \min\{d_k(\rho_k(t)), F_k\}$. Similarly, the flow out of a cell k with density equal to or greater than the critical density $\rho_k(t) \geq \rho_k^c$ is not constrained by the traffic demand and hence $\phi_k(t) = \min\{F_k, s_{k+1}(\rho_{k+1}(t))\}$. A

[1] The effects of congestion spill back from the onramps to the arterials is usually considered to have much worse effects than a congestion on the freeway mainline. Thus, avoiding such a spill back takes priority over avoiding a congestion on the mainline.

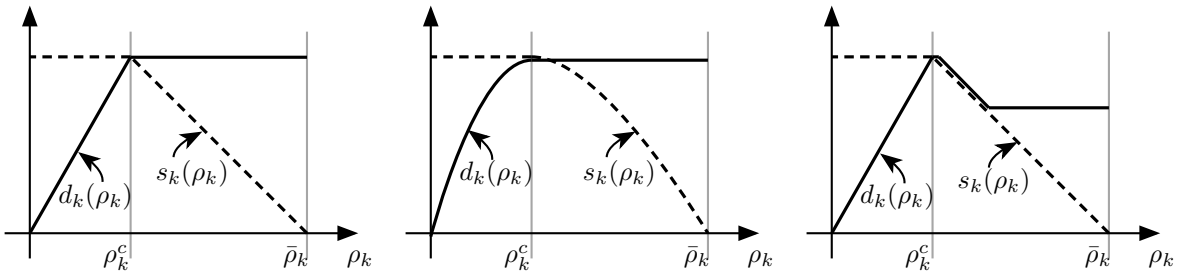

(a) PWA FD (b) Concave FD (c) Nonmonotonic FD

Figure 2: Different shapes of the fundamental diagram (FD) may be desirable in order to approximate real-world data. Figure (a) depicts the traditional PWA version. Figure (b) shows a version with monotonic and concave demand and supply functions, satisfying Assumption 1 for suitable Δt. Clearly, the class of monotonic, concave fundamental diagrams is a generalization of the PWA fundamental diagram. Figure (c) shows a fundamental diagram with non-monotonic demand function, which does *not* satisfy Assumption 1 for any Δt.

CTM freeway model that satisfies Assumption 1 will be called a *monotonic CTM*. The classical, piecewise affine fundamental diagram satisfies this assumption: Here, we have that $d_k(\rho_k) = \min\left\{\bar{\beta}_k v_k \rho_k, \frac{w_k}{\bar{\beta}_k v_k + w_k}\bar{\rho}_k\right\}$ and $s_k(\rho_k) = \min\left\{\frac{w_k}{\bar{\beta}_k v_k + w_k}\bar{\rho}_k, (\bar{\rho}_k - \rho_k)w_k\right\}$ with v_k the free-flow speed and w_k the congestion wave speed. Monotonicity assumptions are trivially satisfied for affine demand and supply functions and the condition on Δt can be recognized as the stability condition $v_k \cdot \Delta t \leq l_k,\ \forall k$ that arises if the CTM is derived as a discretization of the wave PDE using the Godunov scheme. Note that in practice, the congestion-wave speed w_k is significantly lower than the free-flow speed, thus the upper bound in inequality 4b in Assumption 1 is not restrictive. Different shapes of the fundamental diagram encountered in practice are depicted in Figure 2 for illustration.

We are now ready to formulate the main problem. Assume a freeway modeled by the CTM, subject to a demand profile $d_k(t)$ for $k \in \{0, \ldots, n\}$ over a horizon $t \in \{0, \ldots, T-1\}$. By controlling the metering rates, we seek to minimize the total time spent (TTS), given as the sum of the total travel time (TTT),

$$TTT := \Delta t \ \cdot \sum_{t=0}^{T} \sum_{k=0}^{n} l_k \rho_k(t),$$

which is the sum of the travel times of all drivers on the freeway and the total waiting time (TWT),

$$TWT = \Delta t \ \cdot \sum_{t=0}^{T} \sum_{k=0}^{n} q_k(t),$$

the sum of the waiting time of all drivers on the metered onramps. The main problem is therefore given as:

$$\begin{aligned}
\text{minimize} \quad & TTS := TTT + TWT = \Delta t \cdot \sum_{t=0}^{T} \sum_{k=0}^{n} (l_k \rho_k(t) + q_k(t)) && \text{(6a)}\\
\text{subject to} \quad & \rho_k(t+1) = \rho_k(t) + \frac{\Delta t}{l_k} \left(\phi_{k-1}(t) + r_k(t) - \frac{1}{\bar{\beta}_k} \phi_k(t) \right) && \text{(6b)}\\
& q_k(t+1) = q_k(t) + \Delta t \cdot (w_k(t) - r_k(t)) && \text{(6c)}\\
& \phi_0(t) = w_0(t) && \text{(6d)}\\
& \phi_k(t) = \min\{d_k(\rho_k(t)), s_{k+1}(\rho_{k+1}(t))\} && \text{(6e)}\\
& \phi_n(t) = d_n(\rho_n(t)) && \text{(6f)}\\
& 0 \leq r_k(t) \leq \bar{r}_k && \text{(6g)}\\
& 0 \leq q_k(t) \leq \bar{q}_k && \text{(6h)}\\
& \rho_k(0), q_k(0), w_k(t) \text{ given.} && \text{(6i)}
\end{aligned}$$

Note that the metering bounds (3) for time t are equivalent to (6h) at time $t+1$. Problem (6) is a standard problem in traffic control, which has been studied extensively. It is non-convex, because of the nonlinear fundamental diagram (6e). In [6], it is shown that the special case of a piecewise-affine fundamental diagram admits an LP reformulation and hence can be solved efficiently. The case of a concave, but not necessarily PWA fundamental diagrams is briefly discussed in [10], although in a continuous-time setting. Similarly to the PWA case, a convex reformulation is possible.

Remark 1. *In the statement of the main problem* (6)*, we introduce parameters $\bar{r}_k, \bar{q}_k$ and β_k for every cell. In practice, not every cell will be equipped with both an onramp and an offramp and many cells might have neither. The equations* (6) *are general enough to capture all these situations and one can simply select $\bar{r}_k = \bar{q}_k = w_k(t) = 0,\ \forall t$, if no onramp is present in cell k. Similarly, choosing $\beta_k = 0$, which in turn implies that $\bar{\beta}_k = 1$, means no offramp is present in cell k.*

3 A distributed controller

The problem of minimizing TTS represents the global perspective, in which we optimize the whole system over the complete horizon. By contrast, one might also seek to optimize the here-and-now performance. This idea can be formalized by introducing the Total Travel Distance (TTD), defined as

$$TTD(t) := \Delta t \cdot \sum_{k=1}^{n} l_k \phi_k(t),$$

which is simply the total distance traveled by all drivers on the mainline within time interval t. In this section, we formulate an one-step look-ahead controller, which maximizes TTD for the next time step in a greedy fashion:

$$\begin{aligned}
\text{maximize} \quad & TTD(t+1) = \Delta t \cdot \sum_{k=1}^{n} l_k \phi_k(t+1) && \text{(7a)}\\
\text{subject to} \quad & \rho_k(t+1) = \rho_k(t) + \frac{\Delta t}{l_k} \left(\phi_{k-1}(t) + r_k(t) - \frac{1}{\bar{\beta}_k} \phi_k(t) \right) && \text{(7b)}\\
& q_k(t+1) = q_k(t) + \Delta t \cdot (w_k(t) - r_k(t)) && \text{(7c)}\\
& \phi_0(t+1) = w_0(t+1) && \text{(7d)}\\
& \phi_k(t+1) = \min\{d_k(\rho_k(t+1)), s_{k+1}(\rho_{k+1}(t+1))\} && \text{(7e)}\\
& \phi_n(t+1) = d_n(\rho_n(t+1)) && \text{(7f)}\\
& 0 \leq r_k(t) \leq \bar{r}_k && \text{(7g)}\\
& 0 \leq q_k(t+1) \leq \bar{q}_k && \text{(7h)}\\
& \rho_k(t), q_k(t), w_k(t) \text{ given.} && \text{(7i)}
\end{aligned}$$

It is straightforward to show that the following distributed feedback controller provides a (non-unique) explicit solution to this optimization problem. The explicit, feedback solution requires perfect model knowledge, but it does not rely on any online-optimization or traffic demand prediction:

Lemma 1. *An explicit solution to the one-step-ahead optimal control problem* (7) *is given by the following feedback policy:*

$$r_k^*(t) := \left[\frac{l_k}{\Delta t} \left(\rho_k^c - \rho_k(t) \right) + \frac{\phi_k(t)}{\bar{\beta}_k} - \phi_{k-1}(t) \right]_{\max\left\{0, \frac{1}{\Delta t}(q_k(t) - \bar{q}_k) + w_k(t)\right\}}^{\min\left\{\bar{r}_k, \frac{1}{\Delta t} q_k(t) + w_k(t)\right\}} \qquad \forall k \in \{1, \dots, n\}. \tag{8}$$

Proof. Consider an arbitrary flow $\phi_k(t+1)$, $k \in \{1, \dots, n-1\}$. It is easy to see that it only depends on the ramp metering rates in the adjacent cells k and $k+1$ at time t, since we consider a one-step-ahead control problem. More precisely, it depends on the traffic demand $d_k(\rho_k(t))$ and the supply of free space $s_{k+1}(\rho_{k+1}(t))$. Consider the problem of maximizing this flow

$$\begin{aligned} \max_{r(t)} \ \phi_k(t+1) &= \max_{r(t)} \ \min\{d_k(\rho_k(t+1)), s_{k+1}(\rho_{k+1}(t+1))\} \\ &\leq \min\Big\{ \underbrace{\max_{r(t)} \ d_k(\rho_k(t+1))}_{(1)}, \ \underbrace{\max_{r(t)} \ s_{k+1}(\rho_{k+1}(t+1))}_{(2)} \Big\} \end{aligned}$$

alone. It turns out that the policy (8) maximizes both terms in the previous equation. In order to show this, we resort to a case distinction:

(i) If $r_k^*(t)$ does not saturate at the upper bound, it follows that $r_k^*(t) \geq \frac{l_k}{\Delta t} \left(\rho_k^c - \rho_k(t) \right) + \frac{\phi_k(t)}{\beta_k} - \phi_{k-1}(t)$ and hence $\rho_k(t+1) = \rho_k(t) + \frac{\Delta t}{l_k} \left(\phi_{k-1}(t) + r_k^*(t) - \frac{1}{\beta_k} \phi_k(t) \right) \geq \rho_k^c$. Therefore, $d_k(\rho_k(t+1)) = d_k(\rho_k^c)$ and the first term is maximized.

(ii) Otherwise, recall that $d_k(\cdot)$ is nondecreasing. Since $r_k^*(t)$ saturates at the upper bound w.r.t (7g) and (7h) of the feasible range, the first term is maximized.

Similarly, we can analyze the effects of the metering rate at cell $k+1$:

(i) If $r_{k+1}^*(t)$ does not saturate at the lower bound, it follows that $r_{k+1}^*(t) \leq \frac{l_{k+1}}{\Delta t} \left(\rho_{k+1}^c - \rho_{k+1}(t) \right) + \frac{\phi_{k+1}(t)}{\bar{\beta}_{k+1}} - \phi_k(t)$ and hence $\rho_{k+1}(t+1) = \rho_{k+1}(t) + \frac{\Delta t}{l_{k+1}} \left(\phi_k(t) + r_{k+1}^*(t) - \frac{1}{\bar{\beta}_{k+1}} \phi_{k+1}(t) \right) \leq \rho_{k+1}^c$. Therefore, $s_{k+1}(\rho_{k+1}(t+1)) = s_{k+1}(\rho_{k+1}^c)$ and the second term is maximized.

(ii) Otherwise, recall that $s_{k+1}(\cdot)$ is nonincreasing. Since $r_{k+1}^*(t)$ does saturate at the lower bound of the feasible range, the second term is maximized.

Since both the first and the second term are maximized, we conclude that the proposed feedback law maximizes $\phi_k(t+1)$, for all $k \in \{1, \dots, n-1\}$. The case of $\phi_n(t+1)$ is similar, except that the second term is not present. Also $\phi_0(t+1)$ does not depend on the metering rates. All flows are jointly maximized and therefore, TTD is maximized as well. □

This controller aims at moving the local density to the critical density as fast as possible and in that sense, it is very similar in spirit to many existing and practically successful ramp metering strategies, most notably ALINEA [15]. In the following, we will be referring to this one-step-ahead optimal controller as the (distributed) *best-effort controller*. There has been speculation in [26] on whether a control policy similar to the feedback law (8) minimizes TTS globally and over the complete horizon. We will present two counterexamples showing that this is not necessarily the case in all scenarios.

Example 1 (Lower bound saturation)**.** *Consider a two-cell freeway as depicted in Figure 3, with a metered onramp at the second cell and an offramp with a large split ratio at the first cell, in this example $\beta_1 = 0.8$. Some traffic demand is present at the onramp in the beginning, but a spike in demand is arriving on the mainline with some time delay. The situation is sketched in Figure 3a. Because of the large split ratio at*

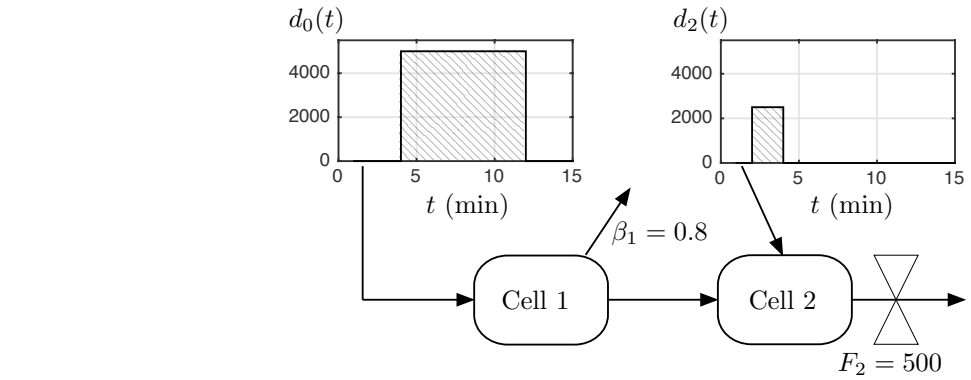

(a) Freeway topology and demand patterns

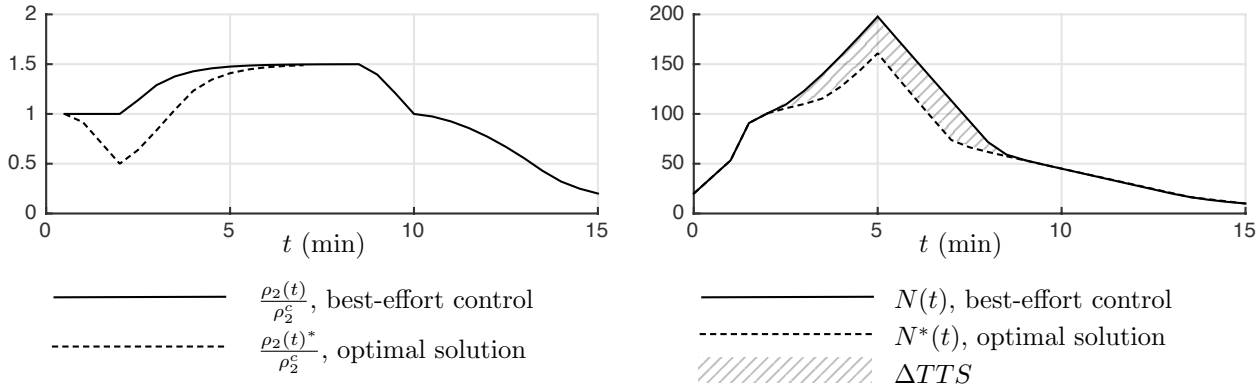

(b) Traffic evolution

Figure 3: In case of a spike in demand, it might be advisable to preemptively reduce the local density at a bottleneck below the critical density, in oder to accomodate (parts of) the traffic wave in the free space and avoid spill back of congestion. The variables $N(t)$ and $N^*(t)$ represent the total number of cars on the freeway and at the onramps, so $N(t) := l_1\rho_1(t) + l_2\rho_2(t) + q_2(t)$ and likewise for $N^*(t)$. Therefore, the savings, i.e., the difference in TTS between the two controllers, are proportional to the highlighted region.

the offramp, a backlog of congestion into the first cell severely reduces the total discharge flows and hence increases the TTT. Once the spike in demand arrives, the constraint $0 \leq r_k(t)$ *becomes active. However, cars already admitted to the freeway from the onramp can not be retracted to the onramp queue. For suitably chosen parameters, the optimal policy is to preemptively reduce the density in the second cell below the critical density, as depicted in Figure 3b. The resulting reduction in outflow from the mainline is more than compensated by the increased discharge from the offramp. The demand is piecewise constant:* $d_0(t) = 5000$ *for* $4 \leq t \leq 12min$, $d_0(t) = 0$ *otherwise and* $d_2(t) = 2200$ *for* $3 \leq t \leq 4min$, $d_2(t) = 0$ *otherwise. The parameters are chosen as* $l_1 = l_2 = 1km$, $v_1 = v_2 = w_1 = w_2 = 100km/h$, $\rho_1^c = 100$*(cars)/km,* $\rho_2^c = 10$*(cars)/km,* $\bar{\rho}_1 = 200$*(cars)/km,* $\bar{\rho}_2 = 20$*(cars)/km,* $F_1 = 1000$*(cars) and* $F_2 = 500$*(cars). Note that the parameter values have been chosen to amplify the suboptimality of the policy for illustration purposes, without considering whether such parameters are realistic.*

Conversely, we can also construct an example in which the upper bound on the ramp metering rate prevents optimality of the local feedback controller:

Example 2 (Upper bound saturation)**.** *Consider a one cell freeway with a metered onramp, as sketched in Figure 4a. Some traffic demand is present at the onramp. A spike in mainline demand arrives at the beginning of the considered time interval, but afterwards, the mainline demand decays to zero. In case of local feedback, the initial spike in mainline demand causes a congestion and hence local feedback will use ramp metering to hold cars back on the queue. But when the mainline density decays again, ramp metering*

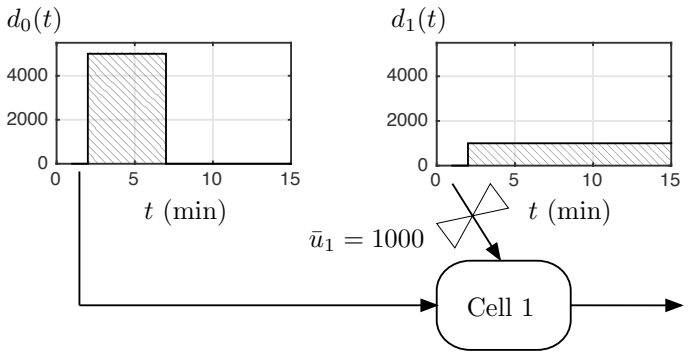

(a) Freeway topology and demand patterns

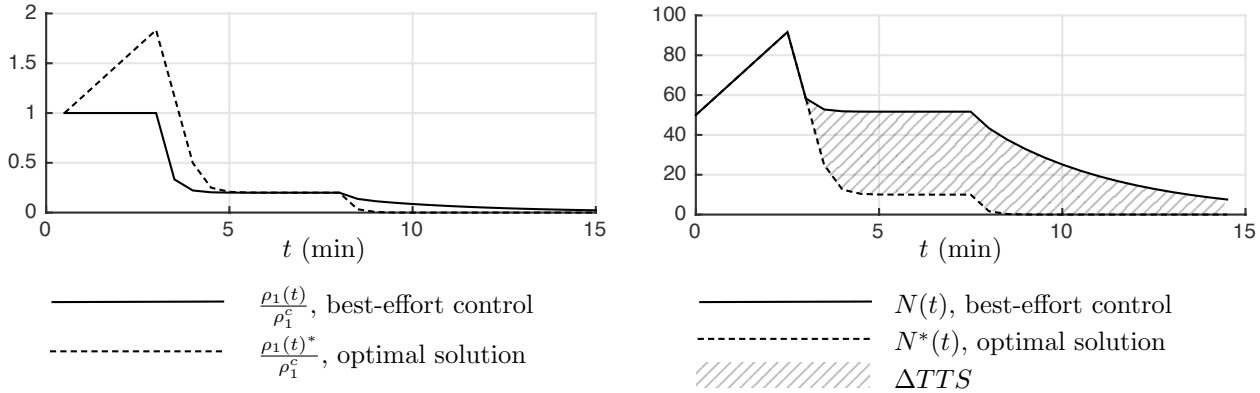

(b) Traffic evolution

Figure 4: If no spill back of the congestion is possible, it might be advisable (in the monotonic CTM) to allow a congestion to form immediately upstream of a bottleneck (highlighted in the upper plot of Figure 4b). The variables $N(t)$ and $N^*(t)$ represent the total number of cars on the freeway and at the onramps, so $N(t) := l_1\rho_1(t) + q_1(t)$ and likewise for $N^*(t)$. Therefore, the savings, i.e., the difference in TTS between the two controllers, are proportional to the highlighted region.

will not be able to release cars sufficiently fast to keep the density at the critical density due to inherent limits on the flow from the onramp, which require $r_k(t) \leq \bar{r}_k$. The optimal strategy does not use ramp metering at all and allows for a larger congestion in the beginning, as depicted in Figure 4b. Since there is no offramp, spill back of congestion is not an issue in this scenario. The demand is piecewise constant: $d_0(t) = 5000$ for $0 \leq t \leq 3min$, $d_0(t) = 0$ otherwise and $d_1(t) = 1000$ for $0 \leq t \leq 8min$, $d_1(t) = 0$ otherwise. The parameter values are chosen as $l_1 = 1km$, $v_1 = 100km/h$, $w_1 = 25km/h$, $\rho_1^c = 50(cars)/km$, $\bar{\rho}_1 = 250(cars)/km$ and $F_1 = 5000(cars)$. Again, the parameter values have been chosen such as to amplify the suboptimality of the policy for illustration purposes.

Closer inspection reveals that whether the ramp metering bounds (2) are active or not is essential for deriving a certificate of optimality. Indeed, in Section 4, we derive explicit conditions relating the activation of these constraints to the optimality of the best effort controller.

4 Sufficient optimality conditions

It turns out that even in the presence of controller saturation, we can find sufficient conditions that can be used to verify optimality of a system trajectory, in a minimal-TTS sense. To derive these, we first apply a linear state transformation to the CTM to obtain a system description better suitable for our analysis and show that the closed-loop system comprised of the CTM in the new coordinates and the best-effort controller

is monotonic. Then, we introduce conditions that characterize the state of onramps at individual time steps and show how these conditions, together with monotonicity of the closed loop, ensure global minimization of TTS.

Let us introduce the *throughput* $\Phi_k(t)$, defined as

$$\Phi_k(t) =: \Phi_k(0) + \Delta t \cdot \sum_{\tau=0}^{t-1} \phi_k(\tau).$$

with $\Phi_k(0) := \sum_{j=k+1}^{n} \frac{1}{\bar{\beta}_{(k+1,j-1)}} (l_j \rho_j(0))$ and $\bar{\beta}_{(k,j)} := \prod_{i=k}^{j} \bar{\beta}_i$ if $k \leq j$ and $\bar{\beta}_{(k+1,k)} := 1$. This constant offset accounts for the initial density of the freeway, that is cars that have entered the freeway and travelled to cell k or further before the considered time horizon. This offset is required to express densities in terms of throughput; it does not affect our optimality arguments.. Note that $\Phi_k(t)$ is dimensionless and can be interpreted as the number of cars that have passed cell k. Using this insight, we can we express the throughput directly in terms of the original system states: We first extend the model to include an additional cell with index $n+1$ at the end of the freeway. This cell is defined to have infinite storage capacity and collects all of the flow that leaves the freeway via the mainline. An infinite storage capacity can be formalized by choosing $s_{n+1}(\rho_{n+1}) \equiv +\infty$ such that all of the upstream demand is admitted and $d_{n+1}(\rho_{n+1}) \equiv 0$ such that no car leaves the cell. The purpose of this cell is to assist in bookkeeping of all the cars that have travelled through the freeway and it will therefore *not* be considered in the computation of the Total Travel Time. Note that some cars also leave the freeway via the offramps, but because of the assumption of constant split ratios, we can reconstruct the outflows from the densities in cells $k \in \{1, \dots, n+1\}$. Let us also define the total inflow up to and including time t as $R_k(t) := \Delta t \cdot \sum_{\tau=0}^{t-1} r_k(\tau)$ and the total, external demands as $W_k(t) := q_k(0) + \Delta t \cdot \sum_{\tau=0}^{t-1} w_k(\tau)$. Both quantities are dimensionless and can be interpreted as the number of cars that have entered the freeway or arrived at the onramp, respectively[2]. We can now express the throughputs

$$\Phi_k(t) = \sum_{j=k+1}^{n+1} \frac{1}{\bar{\beta}_{(k+1,j-1)}} \left(l_j \rho_j(t) - R_j(t)\right). \tag{9}$$

as linear functions of the original states and inputs of the CTM. The whole CTM can be expressed equivalently in terms of the aggregated quantities:

$$\left.\begin{aligned} \Phi_k(t+1) \quad &= f_k(\Phi(t), R(t)) \quad && := \Phi_k(t) + \Delta t \ \phi_k(t), \\ \text{with:} \quad & && \\ & \phi_0(t) && = w_0(t), \\ & \phi_k(t+1) && = \min\{d_k(\rho_k(t+1)), s_{k+1}(\rho_{k+1}(t+1))\}, \\ & \phi_n(t) && = d_n(\rho_n(t)) \\ \text{and:} \quad & \rho_k(t) && = \tfrac{1}{l_k}\left(\Phi_{k-1}(t) - \tfrac{1}{\bar{\beta}_k}\Phi_k(t) + R_k(t)\right), \end{aligned}\right\} \forall k \in \{1, \dots, n\} \tag{10}$$

in which the throughputs $\Phi_k(t)$ are the states and the inflows $R_k(t)$ are the inputs. Note that we introduced the shorthand notation $f_k(\Phi(t), R(t))$ for the systems equations. We will also use $f(\cdot,\cdot) := \left[f_1(\cdot,\cdot) \dots f_n(\cdot,\cdot)\right]^\top$. We also need to translate the input constraints (2) and (3), which now read

$$R_k(t-1) \leq R_k(t) \leq R_k(t-1) + \bar{r}_k, \tag{11a}$$

$$W_k(t) - \bar{q}_k \leq R_k(t) \leq W_k(t). \tag{11b}$$

We will refer to the system described by equations (10) and (11) as the *aggregated CTM*. Monotonicity properties will facilitate the analysis of optimal control problems of the aggregated CTM.

Lemma 2. *The systems equations $f_k(\Phi(t), R(t))$ for all $0 \leq k \leq n$ in the aggregated CTM are nondecreasing in the aggregated flows $\Phi(t)$.*

[2]Note however, that the CTM is an averaged model, so neither $R_k(t)$ nor $W_k(t)$ are restricted to integer values.

Proof. Using the definition of the aggregated CTM (10), we can write equivalently

$$\Phi_k(t+1) = \min\left\{\Phi_k(t) + \Delta t\ d_k(\rho_k(t)), \Phi_k(t) + \Delta t\ s_{k+1}(\rho_{k+1}(t))\right\}$$

for $k \in \{1, \dots, n-1\}$. The minimum of monotonic functions is monotonic. We can therefore verify monotonicity of the CTM by checking that both of the functions

$$f_k^{(-)}(\Phi_{k-1}(t), \Phi_k(t)) := \Phi_k(t) + \Delta t\ d_k\left(\frac{1}{l_k}\left(\Phi_{k-1}(t) - \frac{1}{\bar{\beta}_k}\Phi_k(t) + R_k(t)\right)\right),$$
$$f_k^{(+)}(\Phi_k(t), \Phi_{k+1}(t)) := \Phi_k(t) + \Delta t\ s_{k+1}\left(\frac{1}{l_{k+1}}\left(\Phi_k(t) - \frac{1}{\bar{\beta}_{k+1}}\Phi_{k+1}(t) + R_{k+1}(t)\right)\right),$$

are nondecreasing in $\Phi_{k-1}(t), \Phi_k(t)$ and $\Phi_{k+1}(t)$.

(i) To verify monotonicity in $\Phi_{k-1}(t)$, first note that $f_k^{(+)}$ does not depend on $\Phi_{k-1}(t)$, so it is trivially nondecreasing. Furthermore, $\rho_k(t)$ is nondecreasing in $\Phi_{k-1}(t)$, since by assumption $l_k > 0$. Also, $d_k(\cdot)$ is nondecreasing according to Assumption 1. Recalling that $\Delta t > 0$, we conclude that $f_k^{(-)}$, which is a composition of the previously analyzed functions, is nondecreasing in $\Phi_{k-1}(t)$.

(ii) To verify monotonicity in $\Phi_{k+1}(t)$, first note that $f_k^{(-)}$ does not depend on $\Phi_{k+1}(t)$, so it is trivially nondecreasing. Furthermore, $\rho_k(t)$ is nondecreasing in $\Phi_{k+1}(t)$, since by assumption $l_k > 0$ and $\bar{\beta}_{k+1} > 0$. Also, $s_{k+1}(\cdot)$ is nonincreasing according to Assumption 1. Recalling that $\Delta t > 0$, we conclude that $f_k^{(+)}$, which is a composition of the previously analyzed functions, is nondecreasing in $\Phi_{k+1}(t)$.

(iii) To verify monotonicity of $f_k^{(-)}$ in $\Phi_k(t)$, recall that according to Assumption 1, $d_k(\cdot)$ is Lipschitz continuous, so $|d_k(x + \Delta x) - d_k(x)| \le c_k^d |\Delta x|$. Therefore:

$$\begin{aligned}
&f_k^{(-)}(\Phi_{k-1}(t), \Phi_k(t) + \Delta\Phi) - f_k^{(-)}(\Phi_{k-1}(t), \Phi_k(t)) \\
&\quad = \Delta\Phi + \Delta t \cdot \left[d_k\left(\frac{1}{l_k}\left(\Phi_{k-1}(t) - \frac{1}{\bar{\beta}_k}(\Phi_k(t) + \Delta\Phi) + R_k(t)\right)\right)\right. \\
&\qquad\qquad \left. - d_k\left(\frac{1}{l_k}\left(\Phi_{k-1}(t) - \frac{1}{\bar{\beta}_k}\Phi_k(t) + R_k(t)\right)\right)\right] \\
&\quad \ge \Delta\Phi - \Delta t \cdot c_k^d \cdot \left|\frac{1}{l_k\bar{\beta}_k}\Delta\Phi\right| \\
&\quad \ge \Delta\Phi \cdot \left(1 - \Delta t \cdot \frac{l_k\bar{\beta}_k}{\Delta t} \cdot \frac{1}{l_k\bar{\beta}_k}\right) = 0.
\end{aligned}$$

In the first inequality, we use Lipschitz continuity and in the last inequality, we replace the Lipschitz constant for the demand function with its upper bound from Assumption 1. Monotonicity of $f_k^{(+)}$ in $\Phi_k(t)$ can be shown in a similar way.

Also, the cases $k = 0$ and $k = n$ follow along the same lines. □

Similarly, the dependency of the states on the inputs is characterized by the following relationship:

Lemma 3. *The systems equation $f_k(\Phi(t), R(t))$ for k fixed ($1 \le k \le n-1$) is nondecreasing in input $R_k(t)$ and nonincreasing in input $R_{k+1}(t)$. Also, $f_0(\Phi(t), R(t))$ is nonincreasing in $R_1(t)$ and $f_n(\Phi(t), R(t))$ is nondecreasing in $R_n(t)$.*

The proof of Lemma 3 follows the same ideas as the proof of Lemma 2 and can be found in Appendix A. Next, we will define conditions that will be useful in deriving sufficient optimality conditions for best-effort control.

Definition 1. *A cell k with onramp queue is called* restrictive *at time t if*

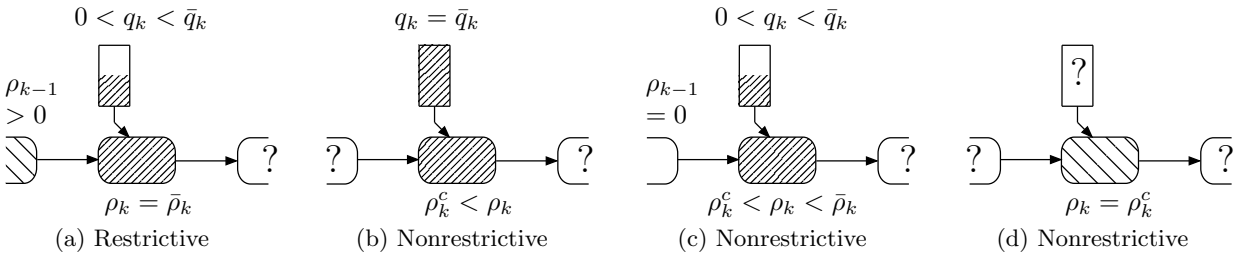

Figure 5: Example situations in which cell k is restrictive or nonrestrictive. A question mark indicates that the corresponding density or ramp occupancy is not relevant for determining if cell k is restrictive or not.

(i) the onramp is not completely full and the upstream flow into the cell is limited by non-maximal supply of free space, i.e., $q_k(t) < \bar{q}_k$ *and* $s_k(\rho_k(t)) \leq d_{k-1}(\rho_{k-1}(t)) \ \wedge \ s_k(\rho_k(t)) < F_{k-1}$

or

(ii) the onramp is not empty and the downstream flow out of the cell is limited by non-maximal demand, i.e., $q_k(t) > 0$ *and* $d_k(\rho_k(t)) \leq s_{k+1}(\rho_{k+1}(t)) \ \wedge \ d_k(\rho_k(t)) < F_k$

Otherwise, we call the cell nonrestrictive.

This definition formalizes the intuitive idea to operate each onramp so as to maximize local mainline flow in the subsequent time step $t + 1$: In case (i), the existence of free space on the onramp indicates that a potential congestion on the mainline, which is equivalent to the flow being restricted by the traffic supply, might have been prevented or at least reduced by keeping additional cars on the onramp. Conversely, the existence of free-flow conditions on the mainline below the maximal flow, as indicated by the restriction of the flow by the traffic demand, raises the question as to why any cars should be held back on the onramp queue. The idea will be illustrated in the following example.

Example 3. *Consider the situations sketched in Figure 5, which exemplify when a cell is restrictive. In all these examples, we assume that* $s_k(\rho_k(t)) > 0$ *if* $\rho_k(t) < \bar{\rho}_k$ *and* $d_k(\rho_k(t)) > 0$ *if* $\rho_k(t) > 0$.

(i) A completely congested cell implies $s_k(\rho_k(t)) = s_k(\bar{\rho}_k) = 0$. *Since the upstream cell is nonempty, it follows that* $s_k(\rho_k(t)) = 0 < d_{k-1}(\rho_{k-1}(t))$. *But even though cell* k *is completely congested, the onramp is not completely filled* $q_k(t) < \bar{q}_k$. *Therefore, cell* k *is restrictive.*

(ii) Cell k *is congested* $\rho_k(t) > \rho_k^c$ *, but in contrast to case (i), the maximal number of cars is stored on the onramp* $q_k(t) = \bar{q}_k$. *Therefore, this cell is nonrestrictive.*

(iii) Cell k *is congested* $\rho_k^c < \rho_k(t) < \bar{\rho}_k$ *and the onramp is not completely filled* $q_k(t) < \bar{q}_k$. *However, in contrast to case (i), the upstream cell* $k + 1$ *is empty, therefore, the congestion in cell* k *does not obstruct the mainline flow* $s_k(\rho_k(t)) > 0 = d_{k-1}(0)$ *and cell* k *is nonrestrictive*

(iv) Cell k *is operating exactly at the critical density. Therefore,* $s_k(\rho_k(t)) = s_k(\rho_k^c) \geq F_{k-1}$ *and* $d_k(\rho_k(t)) = d_k(\rho_k^c) \geq F_k$ *and the cell is nonrestrictive, for arbitrary upstream demand, downstream supply and local ramp occupancy.*

Remark 2. *Definition 1 characterizes cells with onramps. Proofs in the remainder of this section will analyze pairs of adjacent cells, to determine the behavior of the flow between these cells. To avoid unnecessary case distinctions with regard to which of these cells are equipped with onramps and which are not, note that cells without an onramp can still be expressed in the ACTM framework by* $\bar{r}_k = \bar{q}_k = W_k(t) = 0, \ \forall t$, *for all cells* k *without an onramp, exactly in the same way as described in Remark 1 for the CTM. Then constraints* (11) *imply* $R_k(t) = 0, \ \forall t$, *as desired. For such cells* k, *it always holds that* $0 = q_k(t) = \bar{q}_k(t)$ *and therefore, these cells are classified as* nonrestrictive *at all times.*

It is important to note that a cell operating exactly at the critical density ρ_c is always nonrestrictive in the sense of Definition 1: According to Lemma 1, both upstream and downstream flow are jointly maximized at this density. In fact, the best-effort controller defined in said Lemma, which tracks the critical density locally, is able to keep cells nonrestrictive under certain conditions, as explained by the following lemma:

Lemma 4. *Assume that for a freeway controlled by the best effort controller, the onramp at cell k at time t satisfies*

$$0 \leq \left[\frac{l_k}{\Delta t} \left(\rho_k^c - \rho_k(t) \right) + \frac{\phi_k(t)}{\bar{\beta}_k} - \phi_{k-1}(t) \right]_{\frac{1}{\Delta t}(q_k(t)-\bar{q}_k)+w_k(t)}^{\frac{1}{\Delta t}q_k(t)+w_k(t)} \leq \bar{r}_k,$$

i.e., the best-effort policy (8) *is not affected by the constraints* (2)*. Then, cell k is nonrestrictive at time $t+1$.*

Sketch of proof. Note that this condition is sufficient, but not necessary. Sufficiency can be readily verified by plugging the feedback policy in the CTM equations and making a case distinction for each affine piece of the control law. □

We will now use monotonicity of the aggregated CTM to show that throughput is maximized over several time periods for nonrestrictive freeways. For the upcoming analysis, it will be useful to introduce the following notation for the maximal achievable throughput

$$\begin{aligned}
\Phi_k^*(t) := \quad & \max \quad && \Phi_k(t) \\
& \text{subject to} \quad && \Phi(\tau+1) = f(\Phi(\tau), R(\tau)) && \forall \tau \in \{0, \dots, t-1\} \\
& && R_k(\tau) \leq R_k(\tau+1) \leq R_k(\tau) + \bar{r}_k && \forall \tau \in \{0, \dots, t-1\} \\
& && W_k(\tau) - \bar{q}_k \leq R_k(\tau) \leq W_k(\tau) && \forall \tau \in \{0, \dots, t-1\} \\
& && \text{Initial state } \Phi(0) \text{ and } R(0) = \mathbf{0} \text{ given.} && ,
\end{aligned}$$

at a particular time t and cell k.

Lemma 5. *Assume that $\Phi_j(t) = \Phi_j^*(t)$ for $j \in \{k-1, k, k+1\}$ and that the cells k and $k+1$ are nonrestrictive at time t. Then $\Phi_k(t+1) = \Phi_k^*(t+1)$.*

Proof. For notational convenience, let us introduce a relaxation of the set of feasible metering rates

$$\mathcal{R}_k(t) := \{R_k : W_k(t) - \bar{q}_k \leq R_k \leq W_k(t)\} \tag{12}$$

at time t. Note that according to this definition, the metering rates satisfy the constraints arising from the limited space on the onramps (3), but not (necessarily) the additional, constant bounds (2). Also note that the feasible sets for the metering rates $\mathcal{R}_k(t)$ are decoupled in time in the aggregated formulation, i.e., they do not depend on the system state or previous actions. In the following, we will also use the shorthand notation $\mathcal{R}(t) := \otimes_{k=1}^n \mathcal{R}_k(t)$. Now, we can write the optimal throughputs as

$$\begin{aligned}
\Phi_k^*(t+1) \leq \quad & \max \quad && f_k(\Phi(t), R(t)) \\
& \text{subject to} \quad && \Phi(\tau+1) = f(\Phi(\tau), R(\tau)) && \forall \tau \in \{0, \dots, t-1\} \\
& && W_k(\tau) - \bar{q}_k \leq R_k(\tau) \leq W_k(\tau) && \forall \tau \in \{0, \dots, t-1\} \\
& && \text{Initial state } \Phi(0) \text{ and } R(0) = \mathbf{0} \text{ given.} \\
= \quad & \max_{R \in \mathcal{R}(t)} \quad && f_k(\Phi^*(t), R).
\end{aligned}$$

Note that we only have an inequality in the first step, since we operate with a relaxation of the feasible set of inputs. This ensures that the constraints become decoupled in time. Then, we use monotonicity of $\Phi_k(t+1) = f_k(\Phi(t), R(t))$ in the throughputs $\Phi(t)$ to obtain the final equality. Using this preliminary result and the fact that cells k and $k+1$ are nonrestrictive at time t, we will now show that also $\Phi_k(t+1) \geq \Phi_k^*(t+1)$ and hence $\Phi_k(t+1) = \Phi_k^*(t+1)$.

Cell k is nonrestrictive by assumption and therefore, it satisfies either

(A) $d_k(\rho_k(t)) > s_{k+1}(\rho_{k+1}(t)) \ \vee \ d_k(\rho_k(t)) \geq F_k$ or

(B) $q_k(t) = 0$

or both, according to Definition 1. Similarly, cell $k+1$ is also nonrestrictive and satisfies either

(C) $s_{k+1}(\rho_{k+1}(t)) > d_k(\rho_k(t)) \ \vee \ s_{k+1}(\rho_{k+1}(t)) \geq F_k$ or

(D) $q_{k+1}(t) = \bar{q}_{k+1}$

or both. We proceed with a case distinction, depending on which of these conditions are satisfied for cell k and cell $k+1$, respectively:

(i) Assume (A) and (C) hold, that is, the flow $\phi_k(t)$ is neither limited by submaximal supply or submaximal demand. It follows that $\phi_k(t) = \min\{d_k(\rho_k), F_k, s_{k+1}(\rho_{k+1})\} = F_k$ and hence

$$\begin{aligned}\Phi_k(t+1) &= \Phi_k^*(t) + \Delta t \ \cdot F_k \\ &\geq \max_{R \in \mathcal{R}(t)} f_k(\Phi^*(t), R) \\ &= \Phi_k^*(t+1).\end{aligned}$$

(ii) Assume (B) and (D) hold, that is, the onramp in cell k is empty and the onramp in cell $k+1$ is full. The first condition implies that $R_k(t) = W_k(t)$, according to equation (11b). Conversely, the second condition implies that $R_{k+1}(t) = W_{k+1}(t) - \bar{q}_{k+1}$. It follows that

$$\begin{aligned}\Phi_k(t+1) &= \Phi_k^*(t) + \Delta t \ \cdot \min\{d_k(\rho_k), s_{k+1}(\rho_{k+1})\} \\ &= \Phi_k^*(t) + \Delta t \ \cdot \min\left\{d_k\Big(\rho_k\big(\Phi^*(t), W_k(t)\big)\Big), s_{k+1}\Big(\rho_{k+1}\big(\Phi^*(t), W_{k+1}(t) - \bar{q}_{k+1}\big)\Big)\right\} \\ &= \Phi_k^*(t) + \Delta t \ \cdot \min\left\{d_k\Big(\rho_k\big(\Phi^*(t), \max_{R \in \mathcal{R}_k(t)} R\big)\Big), s_{k+1}\Big(\rho_{k+1}\big(\Phi^*(t), \min_{R \in \mathcal{R}_{k+1}(t)} R\big)\Big)\right\} \\ &\geq \max_{R \in \mathcal{R}(t)} f_k(\Phi^*(t), R) \\ &= \Phi_k^*(t+1).\end{aligned}$$

Here, we use the lower and upper bounds on the aggregated ramp metering rates $R_k(t)$ according to the definition of $\mathcal{R}_k(t)$ in equation (12). Finally, the inequality holds because the throughput $\Phi_k(t+1)$ function is nondecreasing in $R_k(t)$ and nonincreasing in $R_{k+1}(t)$, according to Lemma 3.

(iii,iv) In the third case, assume that (A) and (D) hold, whereas in the fourth case, assume that (B) and (C) hold. The derivations to show that $\Phi_k(t+1) \geq \Phi_k^*(t+1)$ can easily be constructed by combining parts from cases (i) and (ii).

All cases compatible with Definition 1 have been verified and the proof has thus been completed. □

A maximization of TTD leads to a minimization of the total discharge flows at every time instant, which in turn corresponds to a minimization of TTS over the whole horizon, as we will show next.

Theorem 1. *Assume that every cell $k \in \{1, \ldots, n\}$ of a freeway is nonrestrictive, for the entire horizon $t \in \{1, \ldots, T-1\}$. Then TTS is minimized.*

Proof. The initial conditions are assumed to be fixed, so $\Phi_k^*(0) = \Phi_k(0)$, for all k. Because Definition 1 holds for every cell in every time step, we can apply Lemma 5 for every cell and $t = 1$, yielding $\Phi_k(1) = \Phi_k^*(1)$ for all k. Employing induction, we can proceed in the same manner to show that $\Phi_k(t) = \Phi_k^*(t)$ over the complete control horizon. Thus, throughput is maximized jointly for every cell and every step.

It remains to be shown that joint maximization of all throughputs implies minimization of TTS. To do so,

$$TTT(t) = \Delta t \cdot \sum_{k=1}^{n} l_k \rho_k(t) = \Delta t \cdot \left(\Phi_0(t) - \Phi_n(t) + \sum_{k=1}^{n} \left(R_k(t) - \frac{\beta_k}{\bar{\beta}_k} \Phi_k(t)\right)\right)$$

and

$$TWT(t) = \Delta t \cdot \sum_{k=1}^{n} q_k(t) = \Delta t \cdot \sum_{k=1}^{n} \left(W_k(t) - R_k(t) \right)$$

have to be expressed in terms of the aggregated variables. If we sum according to the definition of TTS, we find

$$\begin{aligned} TTS &= \sum_{t=0}^{T} TTT(t) + TWT(t) \\ &= \Delta t \cdot \sum_{t=0}^{T} \left(\Phi_0(t) - \Phi_n(t) + \sum_{k=1}^{n} \left(W_k(t) - \frac{\beta_k}{\bar{\beta}_k} \Phi_k(t) \right) \right). \end{aligned}$$

Analyzing the sign of the coefficients yields the desired result

$$\begin{aligned} \text{minimize } TTS &= \Delta t \cdot \sum_{t=0}^{T} \left(\Phi_0(t) - \max\left\{ \Phi_n(t) \right\} + \sum_{k=1}^{n} \left(W_k - \underbrace{\frac{\beta_k}{\bar{\beta}_k}}_{\geq 0} \max\left\{ \Phi_k(t) \right\} \right) \right) \\ &= \Delta t \cdot \sum_{t=0}^{T} \left(W_0(t) - \Phi_n^*(t) + \sum_{k=1}^{n} \left(W_k(t) - \frac{\beta_k}{\bar{\beta}_k} \Phi_k^*(t) \right) \right). \end{aligned}$$

All minimizations and maximizations in the previous equations are to be understood as an optimization over the set of feasible ramp metering patterns, with respect to the fixed initial condition and traffic demands and the CTM system model. Note that $\bar{\beta}_k \in (0, 1]$ for all k by definition of the split ratios. The last equality confirms that TTS is indeed minimized by maximal $\Phi_k^*(t)$ due to an entirely nonrestrictive freeway and thus concludes the proof. □

It is important to keep in mind that Definition 1 provides only *sufficient* optimality conditions. In particular, it is possible that, depending on the freeway parameters and the demand profile, there does not exist a policy which satisfies the given optimality conditions. It also becomes clear that the difficulties in solving the main problem (6) hinge mainly on the ramp metering bounds (2), as the following result states:

Corollary 1. *Assume local ramp metering rates in cell k can be chosen as*

$$r_k(t) = \left[\frac{l_k}{\Delta t} \left(\rho_k^c - \rho_k(t) \right) + \frac{\phi_k(t)}{\bar{\beta}_k} - \phi_{k-1}(t) \right]_{\frac{1}{\Delta t} q_k(t) + d_k(t)}^{\frac{1}{\Delta t}(q_k(t) - \bar{q}_k) + d_k(t)}$$

for all $k \in \{1, \ldots, n\}$ and all $t \in \{0, \ldots, T\}$, i.e., the ramp metering bounds (2) are not support constraints. Then, the local feedback policy minimizes TTS over the whole horizon.

This follows immediately from Theorem 1 and Lemma 4.

5 Application

We consider a congestion prone freeway in the vicinity of Grenoble, France [5]. The total length of this freeway stretch, the so-called Rocade Sud, is 11.8km, out of which we consider 10.45km (exluding short sections in the beginning and in the end). The freeway has 7 offramps in total and 10 onramps, which will be subject to ramp metering in the future. The topology is depicted in Figure 6. The freeway has been equipped with loop detectors. Traffic data are reported to a control center every 15 seconds. In this case study, the freeway is modeled by the CTM, with one cell per mainline sensor location. The parameters of the model are reported in the Appendix B.

(a) Annotated map of the *Rocade Sud*, Grenoble. Circles represent the approximate location of the onramps, offramps and sensors. Map data ©2015 Google

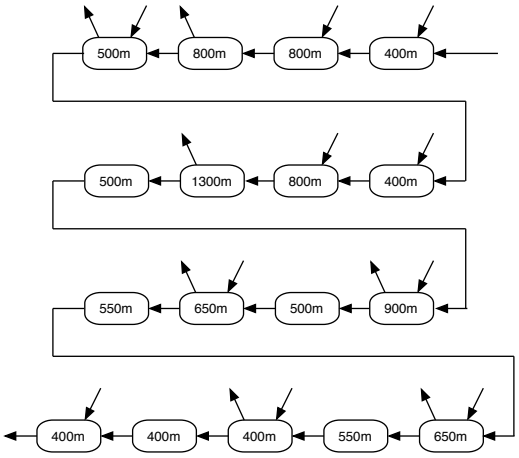

(b) Topology of the CTM modeling the the *Rocade Sud*, with onramps and offramps. Boxes represent the cells of the CTM.

Figure 6: Topology of the *Rocade Sud*, Grenoble

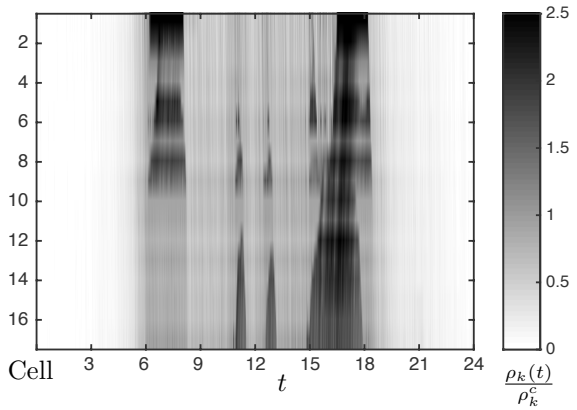

(a) No ramp metering

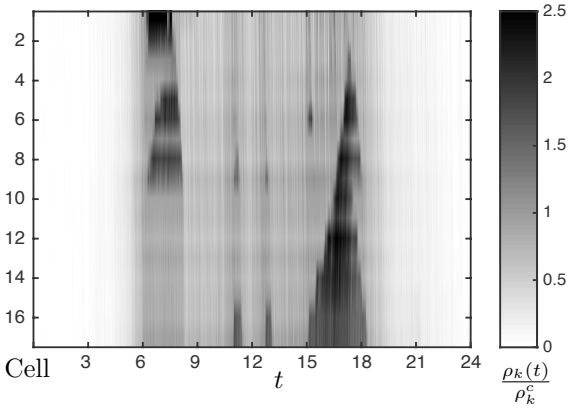

(b) Optimal ramp metering

Figure 7: Partial simulation results of the Grenoble freeway and traffic demands of April, 14th, 2014. Depicted are the mainline densities without ramp metering, and with optimal ramp metering. Because of the limited space on the onramps, it is not possible to prevent congestion altogether, but the improvement is clearly visible.

Since ramp metering has not yet been installed, we can obtain the traffic demand profiles simply from the onramp- and mainline inflows to the system. For the following case study, we consider data from 5 weeks in March, April and June 2014, corresponding to 35 days in total[3]. For each day, we simulate the evolution of traffic using the CTM and best-effort control and report the TTS. For comparison, we also pose the finite horizon optimal control problem over every day, assuming perfect prediction of demand. Employing the results of [6], which derives an equivalent LP reformulation of the optimal control problem, we can compute the optimal trajectories. We are interested in two main questions:

- How often are the (local) optimality conditions violated, i.e., how often are cells restrictive in the sense of Definition 1, over the course of each day?
- How do the travel times under best-effort control compare to the theoretical best-case under predictive optimal control?

5.1 Performance

To establish a baseline for the maximal potential improvement possible, we first compare the open-loop performance, i.e., TTS without ramp metering, to the globally optimal solution. We then analyze the trajectories obtained for best effort control, with particular emphasis on how often cells behave restrictive and therefore, not optimal, and the differences in TTS between best-effort control and the globally optimal solution.

Congestion patterns for a typical day (14.04.2014) are presented in Figure 7, for the uncontrolled freeway and for the freeway under ramp metering. The complete results are summarized in Figure 9. It can immediately be seen that (optimal) ramp metering indeed reduces TTS in most instances. This is achieved by a reduction in congestion and the spill back thereof, thus increasing the outflows from the offramps. On certain days, no improvement can be achieved by ramp metering. These days are characterized by a low traffic demand, as it is typically encountered on weekends. From real traffic data, one can verify that even the uncontrolled freeway typically does not become congested on these days, so obviously no ramp metering is the best policy.

To quantify the benefits of ramp metering, we relate the savings in TTS to the TTS itself, over all days and obtain average savings of

$$\frac{TTS_{noControl} - TTS_{optimal}}{TTS_{noControl}} \approx 5.38\%.$$

A large part of total TTS is caused by vehicles traveling at free-flow velocity, for which ramp metering does not provide any benefits. Therefore, we chose a second metric and compare the savings in TTS to the total time wasted in congestion and in onramp queues. To this end, we define the TFT (Total free-flow time) as the TTS achieved for a hypothetical freeway in which all cars instantly enter the mainline after arriving on an onramp and always travel at free-flow speed on the freeway itself. The relative savings in terms of time wasted in congestion and on onramp queues, over all days, amount to

$$\frac{TTS_{noControl} - TTS_{optimal}}{TTS_{noControl} - TFT} \approx 17.71\%.$$

We note that these numbers are similar to the ones reported in [6].

We now simulate the system using the best-effort controller. In a first step, we verify for every cell with an adjacent onramp and every time step if the cell is nonrestrictive according to Definition 1. It turns out that most cells are nonrestrictive for most of the timesteps. More precisely, the day on which violations most often occur is April 09th on which some cells are restrictive at less than 0.4% of all sampling time instances. We use April 14th, 2014 in order to visualize typical traffic patterns for the freeway controlled by ramp metering. In particular, we highlight several time intervals in which an increase in traffic demand occurs and outline if the optimality conditions for the best-effort controller are satisfied or violated (Figure 8).

[3]Data for the full three months are available, however, data from many days are incomplete due to sensor failures. To ensure representative performance evaluation, only weeks for which data are complete for all sensors at days of the respective week are chosen for the case-study.

The example depicts the evolution of the traffic density in cell 4 and the evolution of the queue length at the adjacent onramp. The morning and the evening rush hour periods are easily visible from the data. Outside of these rush hour periods, cell 4 operates in free-flow and there is no onramp queue, which means that the cell is nonrestrictive. The figure also provides a detailed depiction of the rush hour periods. The intervals in which cell 4 is nonrestrictive are highlighted (A,B,C). However, there exists a time interval D during which the mainline becomes congested, while the onramp queue is not completely filled yet. Note that this example was specifically chosen to depict a situation during which a cell becomes restrictive. According to Figure 8a the traffic demand at the onramp at cell 4 originates from the same roundabout as the traffic demand at the next downstream onramp (cell 5). Therefore, the traffic demand is low at both onramps (in comparison to other onramps on the freeway). Thus it takes longer to fill up the onramp queues and cells 4 and 5 are more likely to become restrictive than other cells in this example.

The performance achieved by best-effort control is also depicted in Figure 9. We can see that the performance in terms of the savings in TWT achieved by the best-effort controller is indistinguishable from the optimal one in a plot scaled according to the absolute values of the savings. A closer look comparing upper- and lower bounds to the optimal solution reveals that the performance deterioration of the best-effort controller, which amounts to

$$\max_{days}\left\{\frac{TTS_{bestEffort}-TTS_{optimal}}{TTS_{optimal}}\right\}\approx 0.178\%$$

in terms of the time wasted in congestion, is worst on May 13th, 2014. Since the optimality of the best-effort controller depends on the ability of the controller to keep the freeway nonrestrictive, bounds on suboptimality in case of failure to do so are of interest. For a given initial state and demand profile, one can use Corollary 1 to compute a lower bound on the TTS. Recall that the range of admissible ramp metering rates $r_k(t)$, depending on the demand $w_k(t)$ and the queue length $q_k(t)$ is given as

$$\min\left\{0,\frac{1}{\Delta t}\left(\bar{q}_k-q_k(t)\right)+w_k(t)\right\}\leq r_k(t)\leq\min\left\{\bar{r}_k,\frac{1}{\Delta t}q_k(t)+w_k(t)\right\},$$

i.e., the ramp metering rate is constrained by constraints on the queue length and fix bounds on the metering rate. For the purpose of deriving a lower bound, one can formulate a relaxed minimal TTS problem starting from the main problem (6), in which the constant bounds on the ramp metering rates are removed. Employing Corollary 1, we find that the solution to this problem can be obtained efficiently by simulating the system for the given demand pattern, using the best-effort controller.

Conversely, an upper bound on the optimal TTS can be computed efficiently by simulating the best-effort controller and respecting all bounds on the metering rates by saturating the control actions accordingly.

It turns out that by using only these inexpensive simulations to compute upper and lower bounds, we can verify a posteriori that the suboptimality is smaller than 0.2%, without the need to compute the optimal solution exactly, i.e., solve a (potentially expensive) optimization problem.

5.2 Comparision with ALINEA

To demonstrate that the theoretical conclusions drawn from the analysis of the best-effort controller indeed extend to practically relevant ramp metering policies, we compare it numerically to ALINEA [15], a popular decentralized ramp metering policy. ALINEA in its basic form consists of local, anti-windup integral feedback controllers. The metering rates are first computed as integral feedback

$$\tilde{r}_k(t):=r_k(t-1)+K_I\cdot(\rho_k^c-\rho_k(t))$$

in which $K_I:=70/(\rho_k^c\cdot\Delta t)$ is the integral gain recommended in [15]. Then, they are saturated

$$r_k(t)=[\tilde{r}_k(t)]_{\max\left\{0,\frac{1}{\Delta t}(q_k(t)-\bar{q}_k)+d_k(t)\right\}}^{\min\left\{\bar{r}_k,\frac{1}{\Delta t}q_k(t)+d_k(t)\right\}} \tag{13}$$

in the same way as for the local feedback controller. There exists a variety of extensions to this basic controller [18, 23, 25], that introduce coordination between ramps or permit use of different sensor configurations. The

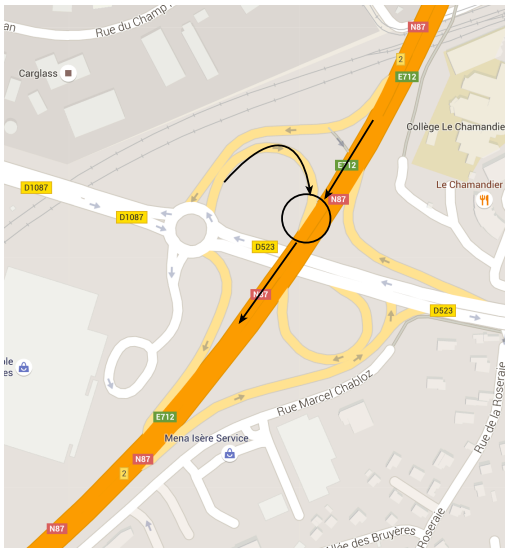

(a) Map of the onramp at cell 4 of the *Rocade Sud*, Grenoble. Note that the onramp is very close to a second onramp, leading to cell 5. Map data ©2015 Google

Symbol in Figure 8c	Density range	Queue length range	Cell k nonrestrictive?
A	$\rho_k \leq \rho_k^c$	$q_k = 0$	Yes
B	$\rho_k = \rho_k^c$	$0 \leq q_k \leq \bar{q}_k$	Yes
C	$\rho_k^c \leq \rho_k$	$q_k = \bar{q}_k$	Yes
D	$\rho_k^c < \rho_k$	$0 < q_k$	Frequently not

(b) Legend to identify time intervals in which the optimality conditions are satisfied (A,B,C) and most likely violated (D). Note that the conditions for classifying a period in group D, i.e., $\rho_k^c < \rho_k$ and $0 < q_k$, are not sufficient for a cell being restrictive, in particular if the critical density is only slightly exceeded, as illustrated in Example 3.

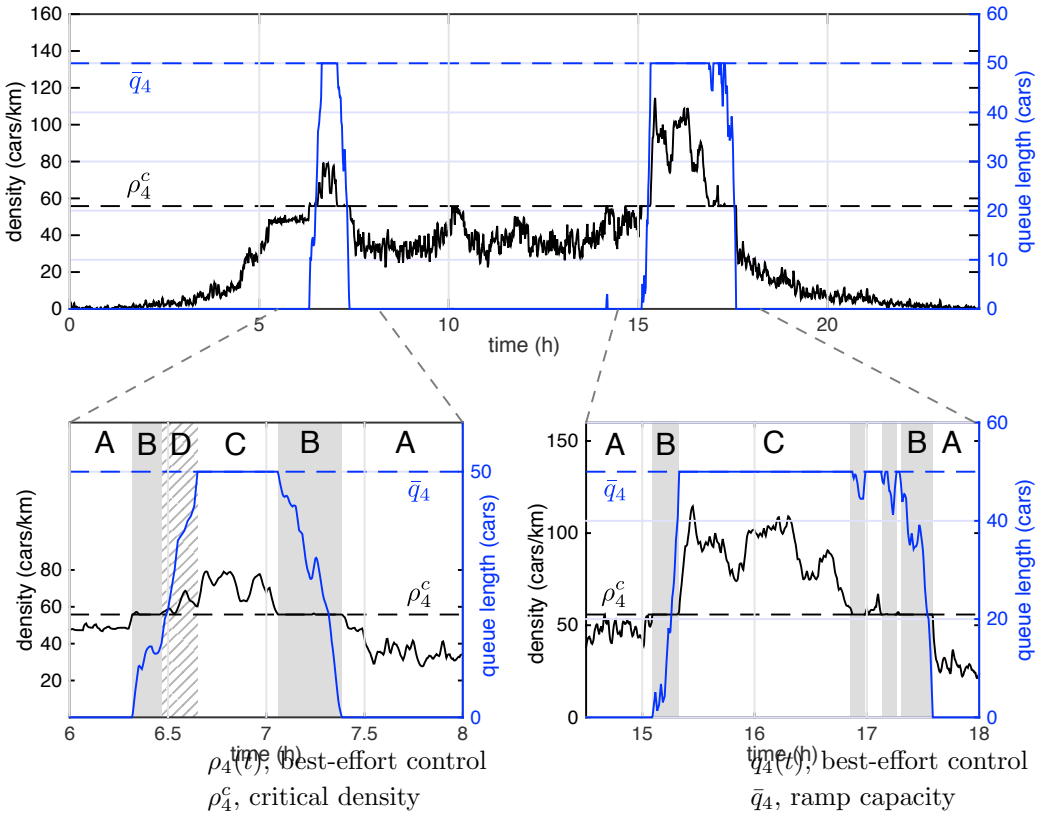

(c) Evolution of traffic density in cell 4 and the queue lengths of the adjacent onramp on April 14th, 2014.

Figure 8: Partial simulation results of the *Rocade Sud*, using the traffic demand of April 14th, 2014.

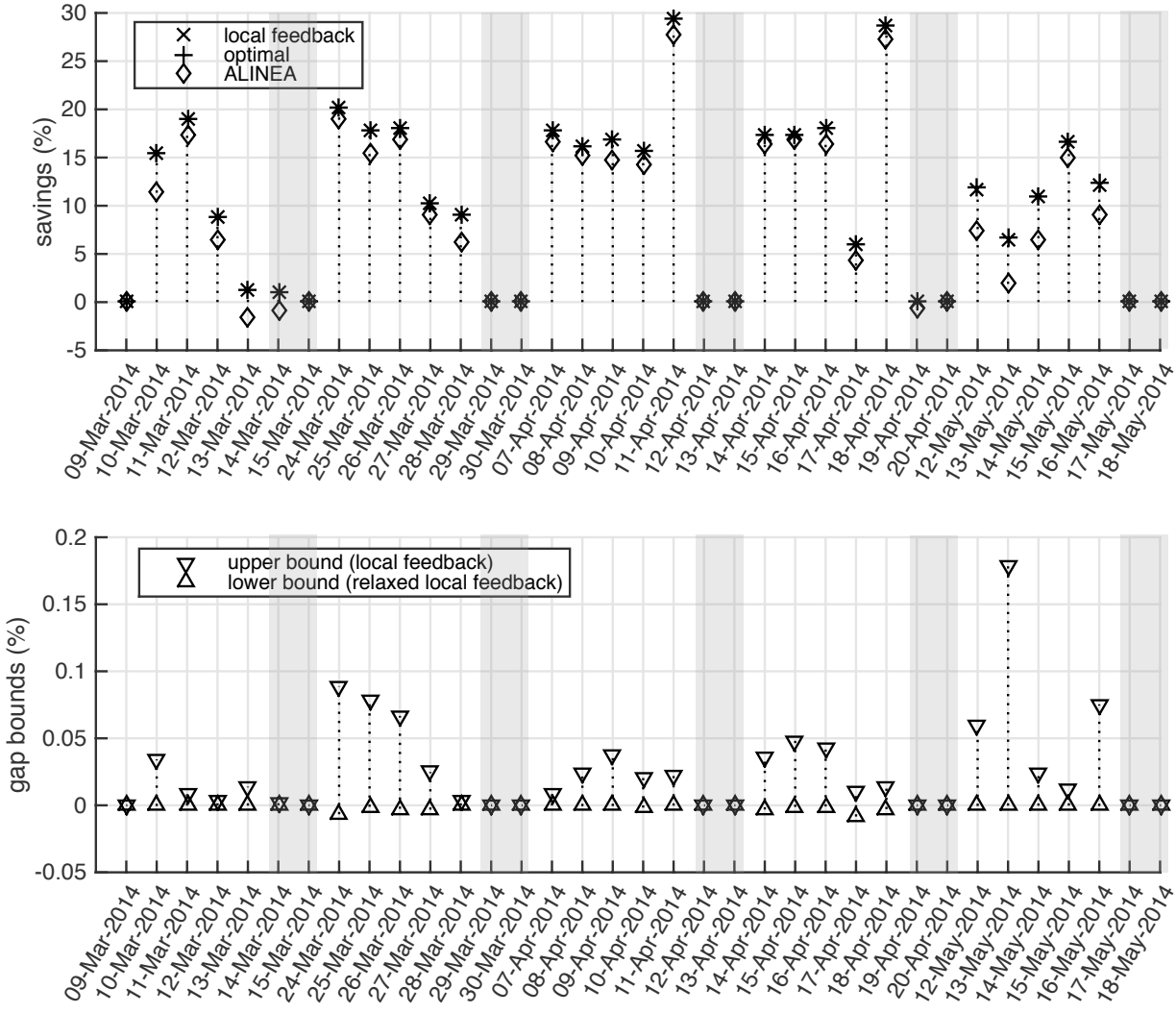

Figure 9: Summary of the TTS achieved by the various controllers, for every day of our case study. In the upper plot, the savings in TTS in relation to the total time in congestion for the uncontrolled freeway (second metric) are depicted. For all days, the performance achieved by local feedback is indistinguishable from the performance of the optimal ramp metering strategy. ALIENA comes close most of the times. On weekends, highlighted in grey, ramp metering does not provide any benefits. In the second plot, we chose a much smaller scale to depict the suboptimality of local feedback, serving as an upper bound, to the optimal TTS (normalized to zero). The performance deterioration is consistently in the range of fractions of percent. We also plot the lower bound on TTS, computed by relaxing the ramp metering constraints, which is even closer to the optimum.

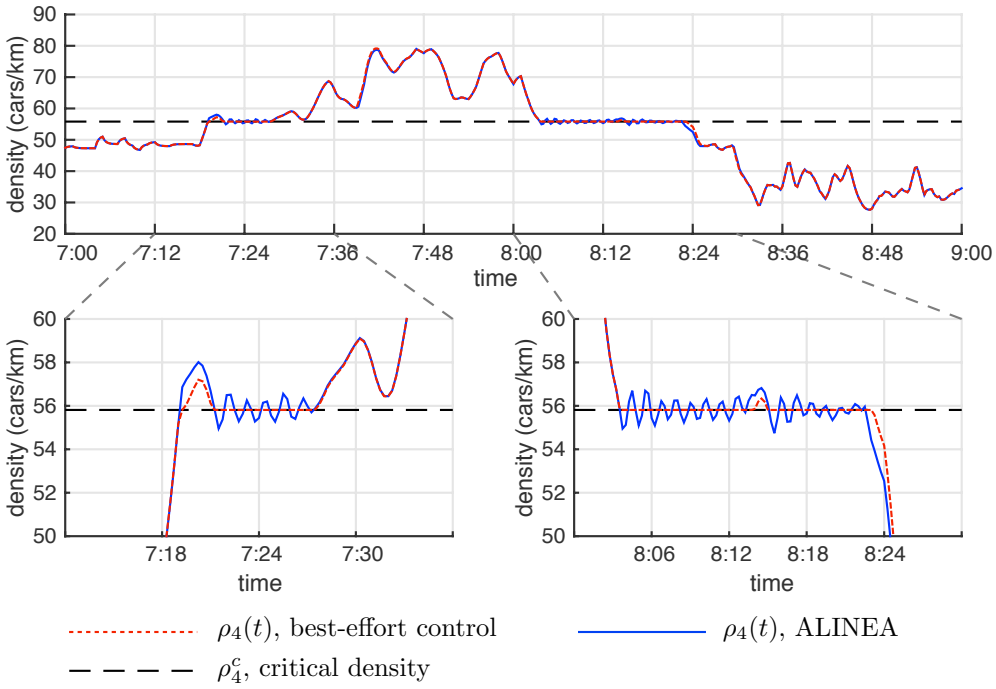

Figure 10: Comparison between the closed-loop trajectories of the local feedback controller and ALINEA for cell 4 during the morning rush hour period of April 14th, 2014. This is the same time interval also depicted in Figure 8, although we focus on the density in this graph.

standard ALINEA controller requires only the critical density as a model parameter. Instead of using model knowledge to estimate and predict traffic demand and supply, this controller uses integral feedback to converge asymptotically to the optimal metering rates in the equilibrium, for constant boundary conditions [22].

Comparing the TTS achieved by the best-effort controller to the freeway controlled by the basic version of ALINEA, we find that the performance deteriorates only slightly, with an average loss of

$$\frac{TTS_{alinea} - TTS_{optimal}}{TTS_{optimal}} = 0.43\%$$

in terms of TTS. A detailed comparison between the TTS achieved by the best-effort controller and ALINEA is also provided in Figure 9. Indeed, for most cases both controllers not only show comparable performance but also show very similar trajectories (see Figure 10). Note that in the top-most figure which depicts the entire rush hour period, differences between the evolution of the densities are hardly visible. They can best be recognized at time intervals during which the controllers do not saturate, i.e., when the density is stabilized at (or close to) the critical density. Here, the lack of perfect model information in ALINEA becomes evident. Changes in upstream- and downstream mainline flow act as disturbances and induce small oscillations in the ALINEA controlled system. By contrast, the best-effort controller law is assumed to have perfect model knowledge and keeps the density exactly at the critical density.

The similarity of the trajectories for both controllers suggests that we can indeed draw conclusions about the behavior of practical ramp metering strategies from our theoretical analysis. In this sense, one should view the slight performance deterioration of ALINEA in comparison to best-effort control as the price one has to pay for not exactly knowing the fundamental diagram in reality.

6 Conclusions

In this work, we have derived sufficient optimality conditions for minimal TTS ramp metering for the monotonic CTM. Based on the analysis, we have defined a suitable distributed, non-predictive feedback

controller motivated as a one-step-ahead maximization of local traffic flows. In simulations using real-world parameters and traffic demands, we demonstrated that the freeway is nonrestrictive most of the time and the controller achieves almost optimal performance. For the sake of keeping the theoretical analysis tractable, we assumed perfect model knowledge which was subsequently used to counteract the model dynamics in the best-effort controller. This assumption is certainly not satisfied in practice and traffic models are typically subject to large uncertainties. However, we demonstrated that the behavior of our proposed controller is very close to that of ALINEA which uses feedback to mitigate the lack of exact model knowledge. Therefore we have verified that our analysis indeed extends to practically successful ramp metering schemes.

We highlight again, that as long as the cells are nonrestrictive, the best-effort controller is optimal and in the CTM framework used in this work, no additional benefit can be realized either by coordination between the ramps or prediction of the traffic demand. The fact that space on the onramps is limited according to constraint (3) does not make coordination between ramps desirable, though it does make ramp metering less effective, of course. In addition, the numerical studies in Section 5 reveal that the conditions for cells being nonrestrictive are satisfied most of the time for a case study using realistic freeway parameters and traffic demands. We achieve results comparable to the global optimal solution with very limited information exchange (only densities of adjacent cells) and without any coordination between the ramps at all. These considerations provide a theoretical explanation for part of the conclusions drawn from practical experience and heuristic considerations in [17].

However, they seem to contradict other practical experience reported in [17], which that suggests that "limited ramp storage space and the requirement of equity ... are the main reasons for coordinated ramp metering". We can resolve this seeming contradiction by recalling that the results on global optimality apply to the monotonic CTM. In practice, there is empirical evidence of a capacity drop at a congested bottleneck. This effect is usually represented by higher-order model such as MetaNet [11], but can also be approximated in a modified CTM [8] by allowing for non-monotonic demand functions, which (slightly) decrease for densities larger than the critical density as depicted in Figure 2c. A congestion in such a model will reduce the bottleneck flow and subsequently decrease densities further downstream, which shows that the dynamic system is no longer monotonic. In a non-monotonic setting, an incentive exists to prevent congestion of a bottleneck, even if there is no danger of spill back of the congestion queue. An important conclusion about the potential benefits of coordinated ramp metering can be drawn from this analysis: coordinated ramp metering may target inefficiencies that result from limited space on the onramps *in conjunction with the nonmonotonic behavior of a congested bottleneck*. Any model-based, coordinated ramp metering strategy therefore must employ a model that is able to reproduce this effect, in order to recognize and avoid it. For example, model-predictive control based on the monotonic CTM and a maximize-TTD or minimize-TTS objective is unlikely to provide any improvements over the presented distributed strategy at all. A heuristic targeting the nonmonotonic effects, such as the addition of a penalty term for the congested region, may serve the same purpose.

Based on these results, two main future research directions seem promising: First, an a-priori quantification of the suboptimality incurred because of infrequent violation of the optimality conditions or because of uncertainty in the knowledge of the fundamental diagram would be helpful. Theoretical bounds on the suboptimality in the presence of a general, not necessarily monotonic CTM would be very helpful, but since no convex reformulation or other efficient, global solution methods for optimal control problems involving the nonmonotonic CTM exist, it is questionable, whether tight bounds can be derived. Instead, the known results on the impact of nonmonotonic behavior can now be used to design control laws for nonmonotonic, realistic freeway models in a more systematic manner by starting from the optimal solution for the monotonic case and specifically targeting the nonmonotonicities with modifications to this baseline control strategy.

Acknowledgements

We are grateful to the Grenoble Traffic Lab at INRIA, Grenoble, France for providing the traffic data used for evaluation.

References

References

[1] Mazen Alamir. *Collaborative Ramp Metering Control: Application to Grenoble South Ring*. PhD thesis, Lund University, Sweden, 2014.

[2] M. Burger, M. Van Den Berg, A. Hegyi, B. De Schutter, and J. Hellendoorn. Considerations for model-based traffic control. *Transportation Research Part C: Emerging Technologies*, 35:1–19, 2013.

[3] Carlos F. Daganzo. The cell transmission model: A dynamic representation of highway traffic consistent with the hydrodynamic theory. *Transportation Research Part B: Methodological*, 28(4):269–287, 1994.

[4] Carlos F. Daganzo. The cell transmission model, part ii: network traffic. *Transportation Research Part B: Methodological*, 29(2):79–93, 1995.

[5] Carlos Canudas de Wit, Fabio Morbidi, Luis Leon Ojeda, Alain Y. Kibangou, Iker Bellicot, and Pascal Bellemain. Grenoble traffic lab: An experimental platform for advanced traffic monitoring and forecasting. *Control Systems, IEEE*, 35(3):23–39, 2015.

[6] Gabriel Gomes and Roberto Horowitz. Optimal freeway ramp metering using the asymmetric cell transmission model. *Transportation Research Part C: Emerging Technologies*, 14(4):244–262, 2006.

[7] Gabriel Gomes, Roberto Horowitz, Alex A Kurzhanskiy, Pravin Varaiya, and Jaimyoung Kwon. Behavior of the cell transmission model and effectiveness of ramp metering. *Transportation Research Part C: Emerging Technologies*, 16(4):485–513, 2008.

[8] Iasson Karafyllis, Maria Kontorinaki, and Markos Papageorgiou. Global exponential stabilization of freeway models. *International Journal of Robust and Nonlinear Control*, 26(6):1184–1210, 2016. rnc.3412.

[9] Michael J. Lighthill and Gerald Beresford Whitham. On kinematic waves ii. a theory of traffic flow on long crowded roads. *Proceedings of the Royal Society of London A: Mathematical, Physical and Engineering Sciences*, 229(1178):317–345, 1955.

[10] Enrico Lovisari, Giacomo Como, Anders Rantzer, and Ketan Savla. Stability analysis and control synthesis for dynamical transportation networks. *arXiv preprint arXiv:1410.5956*, 2014.

[11] Albert Messner and Markos Papageorgiou. Metanet: A macroscopic simulation program for motorway networks. *Traffic Engineering & Control*, 31(8-9):466–470, 1990.

[12] Fabio Morbidi, Luis Leon Ojeda, Carlos Canudas De Wit, and Iker Bellicot. A new robust approach for highway traffic density estimation. In *IEEE European Control Conference (ECC)*, pages 2575–2580, 2014.

[13] Luis L. Ojeda, Alain Y. Kibangou, and Carlos Canudas De Wit. Adaptive kalman filtering for multi-step ahead traffic flow prediction. In *IEEE American Control Conference (ACC)*, pages 4724–4729, 2013.

[14] Markos Papageorgiou, Christina Diakaki, Vaya Dinopoulou, Apostolos Kotsialos, and Yibing Wang. Review of road traffic control strategies. *Proceedings of the IEEE*, 91(12):2043–2067, 2003.

[15] Markos Papageorgiou, Habib Hadj-Salem, and Jean-Marc Blosseville. Alinea: A local feedback control law for on-ramp metering. *Transportation Research Record*, (1320):58–64, 1991.

[16] Markos Papageorgiou and Apostolos Kotsialos. Freeway ramp metering: An overview. In *IEEE Proceedings on Intelligent Transportation Systems*, pages 228–239, 2000.

[17] Ioannis Papamichail, Apostolos Kotsialos, Ioannis Margonis, and Markos Papageorgiou. Coordinated ramp metering for freeway networks–a model-predictive hierarchical control approach. *Transportation Research Part C: Emerging Technologies*, 18(3):311–331, 2010.

[18] Ioannis Papamichail and Markos Papageorgiou. Traffic-responsive linked ramp-metering control. *IEEE Transactions on Intelligent Transportation Systems*, 9(1):111–121, 2008.

[19] Ioannis Papamichail, Markos Papageorgiou, Vincent Vong, and John Gaffney. Heuristic ramp-metering coordination strategy implemented at monash freeway, australia. *Transportation Research Record: Journal of the Transportation Research Board*, 2178(1):10–20, 2010.

[20] Dominik Pisarski and Carlos Canudas-de Wit. Optimal balancing of road traffic density distributions for the cell transmission model. In *Decision and Control (CDC), 2012 IEEE 51st Annual Conference on*, pages 6969–6974. IEEE, 2012.

[21] Paul I Richards. Shock waves on the highway. *Operations research*, 4(1):42–51, 1956.

[22] Marius Schmitt, Paul Goulart, Angelos Georghiou, and John Lygeros. Flow-maximizing equilibria of the cell transmission model. In *Control Conference (ECC), 2015 European*, pages 2634–2639. IEEE, 2015.

[23] Emmanouil Smaragdis, Markos Papageorgiou, and Elias Kosmatopoulos. A flow-maximizing adaptive local ramp metering strategy. *Transportation Research Part B: Methodological*, 38(3):251–270, 2004.

[24] Yorgos J. Stephanedes. Implementation of on-line zone control strategies for optimal ramp metering in the minneapolis ring road. In *Seventh International Conference on Road Traffic Monitoring and Control*, pages 181–184. IET, 1994.

[25] Yibing Wang, Elias B. Kosmatopoulos, Markos Papageorgiou, and Ioannis Papamichail. Local ramp metering in the presence of a distant downstream bottleneck: Theoretical analysis and simulation study. *IEEE Transactions on Intelligent Transportation Systems*, 15(5):2024–2039, 2014.

[26] Lei Zhang and David Levinson. Optimal freeway ramp control without origin–destination information. *Transportation Research Part B: Methodological*, 38(10):869–887, 2004.

[27] Michael H. Zhang and Stephen G. Ritchie. Freeway ramp metering using artificial neural networks. *Transportation Research Part C: Emerging Technologies*, 5(5):273–286, 1997.

[28] Athanasios K. Ziliaskopoulos. A linear programming model for the single destination system optimum dynamic traffic assignment problem. *Transportation science*, 34(1):37–49, 2000.

A Proof of Lemma 3

Proof. As in the proof of Lemma 2, we make use of the fact that we can write the aggregated CTM for $k \in \{1, \dots, n-1\}$ as

$$\Phi_k(t+1) = \min\left\{\Phi_k(t) + \Delta t\ d_k(\rho_k(t)), \Phi_k(t) + \Delta t\ F_k, \Phi_k(t) + \Delta t\ s_{k+1}(\rho_{k+1}(t))\right\}.$$

The minimum function preserves monotonicity of its arguments. We can therefore verify monotonicity of the ACTM by checking that each of the functions:

$$f_k^{(-)}(\Phi_{k-1}(t), \Phi_k(t)) := \Phi_k(t) + \Delta t\ d_k\left(\frac{1}{l_k}\left(\Phi_{k-1}(t) - \frac{1}{\bar{\beta}_k}\Phi_k(t) + R_k(t)\right)\right),$$
$$f_k^{(+)}(\Phi_k(t), \Phi_{k+1}(t)) := \Phi_k(t) + \Delta t\ s_{k+1}\left(\frac{1}{l_{k+1}}\left(\Phi_k(t) - \frac{1}{\bar{\beta}_{k+1}}\Phi_{k+1}(t) + R_{k+1}(t)\right)\right)$$

is nondecreasing in $R_k(t)$ and nonincreasing in $R_{k+1}(t)$.

- To verify that $\Phi_k(t+1)$ is nondecreasing in $R_k(t)$, first note that $f_k^{(+)}$ does not depend on $R_k(t)$ and is therefore trivially nondecreasing in this argument. Furthermore, $\rho_k(t)$ is nondecreasing in $R_k(t)$, since by assumption $l_k > 0$. Also, $d_k(\cdot)$ is nondecreasing according to Assumption 1. Recalling that $\Delta t > 0$, we conclude that $f_k^{(-)}$, which is a composition of the previously analyzed functions, is nondecreasing in $\mathbb{R}_k(t)$.

- To verify that $\Phi_{k+1}(t)$ is nonincreasing in R_{k+1}, first note that $f_k^{(-)}$ does not depend on $R_{k+1}(t)$ and is therefore trivially nonincreasing in this argument. Furthermore, $\rho_{k+1}(t)$ is nondecreasing in $R_{k+1}(t)$, since by assumption $l_k > 0$. Also, $s_{k+1}(\cdot)$ is nonincreasing according to Assumption 1. Recalling that $\Delta t > 0$, we conclude that $f_k^{(+)}$, which is a composition of the previously analyzed functions, is nonincreasing in $R_{k+1}(t)$.

The proof of the cases $k = 0$ and $k = n$ follows along the same lines. □

B Parameter choices

The sensor placement on the real freeway is described in [5]. The topology of the freeway, in particular the lengths l_k of cells of the CTM, can then easily be recovered from publicly available sources, e.g. Google maps. It is important to note that although ramp metering will be installed in the future, it is not in place as of now (November 22, 2016). We report the current lengths of the onramps $\tilde{l}_k^{on}$, but in this work, we chose to increase the onramp queue length to $l_k^{on} = 400$m, a value also used in [6]. This seems justified since installation of ramp metering should go along with the construction of sufficiently long queues to promise any benefits. Note that in the model, we use the dimensionless onramp capacity $\bar{q}_k$, which is the maximal number of cars in the onramp queue. One has $\bar{q}_k = l_k^{on}/8$m, which corresponds to a jam density of 125 (cars)/km (see below the definition of $\bar{\rho}_k$). The maximal onramp flow was chosen as $\bar{r}_k = 1800$ (cars)/h for every onramp, a standard choice corresponding to one car every two seconds. We model the freeway dynamics with the CTM using a PWA fundamental diagram, which is fully characterized by the three parameters v, w and $\bar{\rho}$. The free-flow velocity $v = 90$km/h is equal to the speed limit on the freeway[4]. The jam density is chosen as 250 (cars)/km in every cell. This is a standard choice for a two-lane freeway, related to the average length of vehicles and typical distances between vehicles in standstill. The congestion wave speed was estimated from collected traffic data. Some minor parameter adaptations have been necessary to reproduce typical congestion patterns seen in reality: The maximal flow in section 9 was reduced in comparison to the estimated value, such that this section becomes a bottleneck in rush-hour times, as observed in reality. Furthermore, congestion data from the end of the freeway (sections 15, 16 and 17) are disturbed by what seems to be spill-back effects of the roads downstream of the considered freeway. Since we do not have data about downstream traffic conditions available, we resort to a reasonable estimate of the congestion wave speed and use the value that was identified for section 14. As soon as v, w and $\bar{\rho}$ are chosen, additional parameters like ρ_k^c and F_k can be computed using the standard equations. We assume that the split ratios β_k are constant in time. The values are again estimated from real traffic data. We use a discretization of $\Delta t = 15$s, in accordance with the data transmission interval of the sensors[5]. A summary of all data is given in Table 1, the parameter values that have been changed manually, as described in the previous section, are highlighted by a star *.

[4] On the real freeway, infrastructure to allow for Variable Speed Limits (VSL) is already in place. So far, this capability is only used in case of high air pollution, when the speed limit is lowered to 70km/h. In this work, we do not consider VSL.

[5] The sensors count cars over intervals of 15s and then submit the aggregated data at once.

Table 1: Parameter values of the Grenoble Freeway

cell k	l_k (km)	$\tilde{l}_k^{on}$ (m)	l_k^{on} (m)	v_k (km/h)	$\bar{q}_k$ (cars)	w_k (km/h)	F_k (cars/h)	β_k (%)
1	0.4	100	400*	90	50	21.9555	4412.4572	0
2	0.8	400	400*	90	50	28.1816	4822.1042	0
3	0.8	-	-	90	50	25.3593	4137.386	10.48
4	0.8	120	400*	90	50	21.3061	4137.386	17.63
5	0.5	150	400*	90	50	23.6435	4681.1234	0
6	0.45	120	400*	90	50	25.3959	4481.0999	0
7	0.75	-	-	90	50	23.1183	4481.0999	11.35
8	1.3	-	-	90	50	24.9148	4228.8694	0
9	0.5	300	400*	90	50	21.3992	4000*	10.30
10	0.9	-	-	90	50	23.3808	4292.1031	0
11	0.5	200	400*	90	50	22.2375	4292.1031	16.32
12	0.65	-	-	90	50	25.2238	4497.1729	0
13	0.55	200	400*	90	50	23.1525	4497.1729	10.38
14	0.65	-	-	90	50	26.0173	4950.0238	0
15	0.55	200	400*	90	50	26.0173*	4950.0238	7.94
16	0.45	-	-	90	50	26.0173*	5045.7076	0
17	0.4	60	400*	90	50	26.0173*	5045.7076	0